Chapter 1

Introduction

1 INTRODUCTION

1.1 LAYERED DOUBLE HYDROXIDES

Clays are layered nanostructured materials, widely used as unique additives and fillers in polymeric, cosmetic and pharmaceutical products. For many years they represented the largest and most widely used material. Clay is defined as a hydrous silicate particle less than 2 µm in diameter, composed of silicon, aluminium oxides and hydroxides, as well as structural water. In general, they possess excellent properties, such as low or nil toxicity, biocompatibility and the possibility for use in 'controlled-release' pharmaceutical and cosmetic products. A substantial amount of research has been carried out on the application and characterisation of smectite (cationic) clays (Utracki, 2004; Kumar *et al.*, 2009). Smectite or phyllosilicates are predominately natural clays. However, natural clays have drawbacks such as variability in composition, difficulty in purifying, poor reproducibility of the performance of polymer composites, crystallographic defects that prevent total exfoliation and variable colour (Utraki, 2004). Other layered nanostructured materials, such as layered double hydroxides (LDHs), may be considered as potential alternatives. LDHs possess a higher exchange capacity (typically anionic exchange capacity (AEC) = 0.5 to 6) as compared with cationic clays (cation exchange capacity (CEC) = 0.5–2) (Utraki *et al.*, 2007).

LDHs are referred to as 'hydrotalcite-like' compounds. They are also described as mixed metal hydroxides that consist of positively charged metal hydroxide sheets with metals in different oxidation states. The crystallography of these materials is similar to that of hydrotalcite, with a formula of $Mg_6Al_2(OH)_{16}(CO_3).4H_2O$ (Reichle, 1986). LDHs have various advantages, such as low incidence of impurities since they are synthetic, and a wide variety of metal species and mole ratio compositions can be prepared. However, the high charge density within the interlayer renders LDHs unattractive as they do not easily delaminate or exfoliate in polymers or any media of dispersion. This 'handicap' may be counteracted by a process called *intercalation*. The intercalation process achieves this through the insertion of exchangeable anions, hence reducing the solid-solid interaction within the clay layers. This is essential as the van der Waals interaction between solid surfaces decreases with the square of the separating distance (Utraki, 2004). The process also improves the compatibility of the clay with the polymer matrices in the preparation of

polymer–nanocomposites (Utraki, 2004). The insertion of anions such as surfactants functionalises the clay by converting the hydrophilic nature of the interlayer into a hydrophobic one. Consequently, non-polar and low-water-soluble organic molecules may be absorbed into the interlayer. Various anions have been exchanged within the interlayer, such as halides (Xu & Zeng, 2001), organic anions, e.g. carboxylates, benzenecarboxylates and alkylsulphates (Meyn *et al.*, 1990; Carlino, 1997; Newman & Jones, 1998), polymeric anions (Oriaki *et al.*, 1996), complex anions (Crespo *et al.*, 1997), macrocyclic ligands and their metal derivatives (Robins & Dutta, 1996), iso- and heteropolyoxometalates (Drezdon, 1998) and biochemical anions (Choy, 2004).

In this study the organo-LDHs were synthesised directly from the LDH-CO_3 through a surfactant-mediated one-pot synthesis. The method is convenient (low reaction temperature and relatively short reaction time), environmentally friendly (no toxic solvent used) and economical. Although the method does not entail procedures to exclude carbon dioxide or carbonate, such as working in inert environments, its products are of good crystallinity and have minimal carbonate contamination.

The surfactants of choice in the study are fatty acids or carboxylic acids. Fatty acids are normally unbranched and have an even number of carbon atoms. The anions were chosen because they are readily available and at low cost. Fatty acids are derived from the hydrolysis of animal fat or vegetable oil in aqueous NaOH to yield gylycerol and fatty acids. However, they may be produced synthetically through hydroxycarboxylation of alkenes.

1.2 LDH-BASED POLYMER COMPOSITES

Composite materials make a large contribution to engineering materials in the form of alloys, reinforced concrete and carbon black in vehicle tyres, etc. Biological systems are also good examples that possess a wide variety of composites. The technological world has a constant demand for multifunctional materials. Hence, numerous researchers have embarked on exploring various methods of synthesising and improving materials properties. The main application markets for clay-based polymer nanocomposites are packaging, flame retardants, aerospace and aviation, and the automotive industry. Figure 1.1. shows the

global application market projections for clay-based polymer composites. Growth is predicted in some areas as, well as greater diversity in their application by 2017.

The dispersion of particles with high aspect ratios, such as fibres and platelets in polymeric matrices, together with adequate interfacial adhesion between the filler and polymer, results in improved properties of the polymer matrices. Nanostructured anionic clays such as LDHs impart these properties and are therefore ideal for polymer-clay nanocomposite preparations. The resulting polymeric hybrids exhibit improved gas barrier properties, strength, dimensional stability, flame retardancy and ultraviolet (UV) stability, etc.

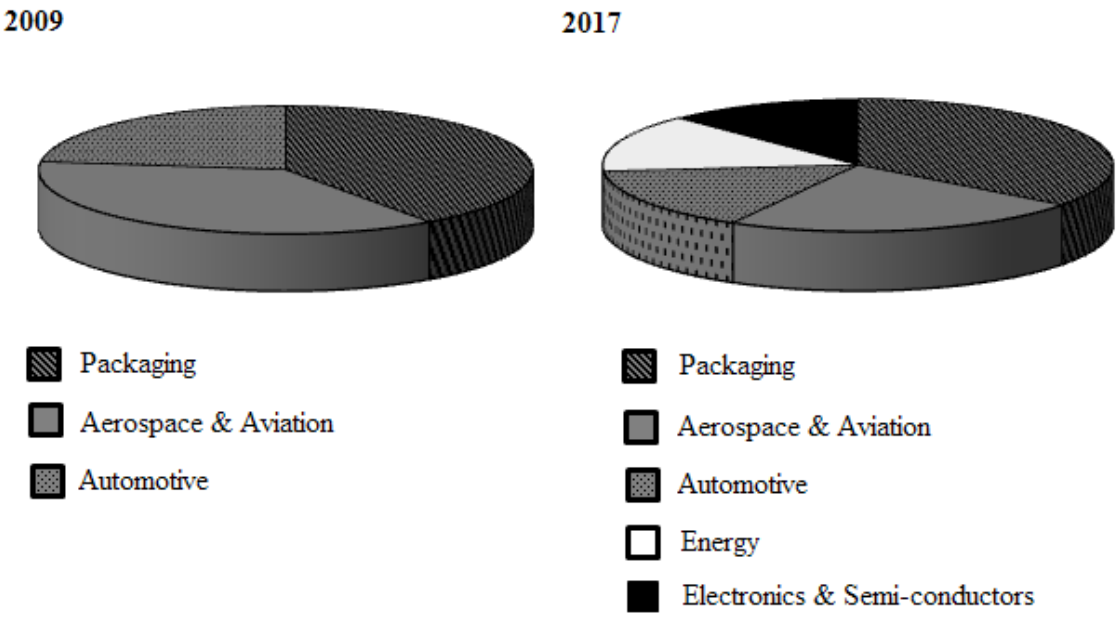

Figure 1.1. Global application market share projections for polymer composites (Adapted from Research and Markets, http://www.researchandmarkets.com)

Surfactant-intercalated LDHs have been reported to exfoliate in polymer matrices and organic solutions (Leroux & Besse, 2001; Khan & O'Hare, 2002; Fischer, 2003). However, the intercalated anions show thermotropic behaviour (Nhlapo *et al.*, 2008; Focke *et al.*, 2010; Moyo *et al.*, 2012). An example of this behaviour is shown in Figure 1.2 where LDH-stearate intercalated above the AEC level melts below typical polymer processing temperatures (120 °C) (Nhlapo *et al.*, 2008). Droplet formation was observed in hot stage optical microscopy, giving a façade of a completely molten LDH-stearate (Nhlapo *et al.*, 2008). This can be attributed to the excess stearate acid exuding and forming a liquid

droplet that surrounds the parent LDH-stearate platelets. However, droplet formation was not observed when the samples were heated in an environmental scanning electron microscope (SEM) because the acid evaporated. This effusion of the excess stearic acid from the bilayer intercalated LDHs proceeds in stages. It starts with the removal of interlayer water and terminates in a monolayer-intercalated clay residue, depending on the temperatures the material is exposed to.

These observations imply that dispersion of LDH-fatty acids in polymer matrices may perhaps not follow the conventional exfoliation or delamination routes (Adachi-Pagano *et al.*, 2000). The exudation of stearic acid may have implications on the processing behaviour and the composite properties (particularly the mechanical properties). Such thermal events are of concern, hence clarity is required as to whether they are advantageous or detrimental to the resultant composite. It was therefore of interest to carry out a comprehensive study on the properties of fatty acid intercalated layered double hydroxides, as well as to follow the micro- and nanopolymer composites obtained therefrom.

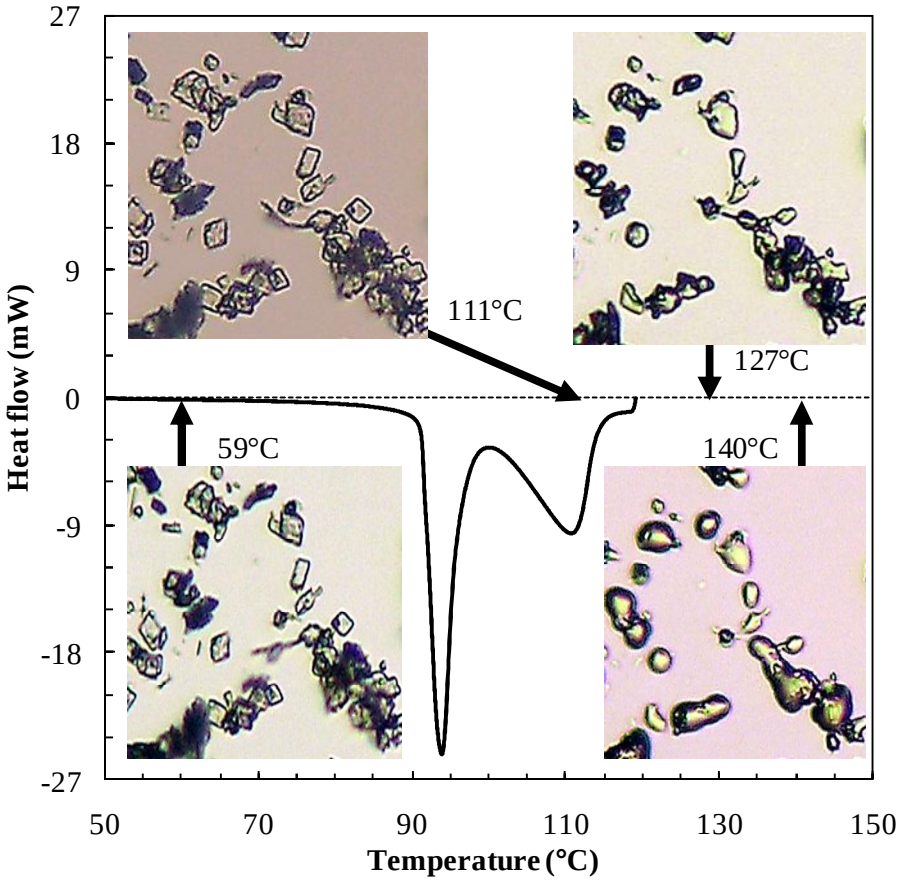

Figure 1.2. Differential scanning calorimetry (DSC) melting endotherm and hot stage microscopy of LDH-stearate (Nhlapo *et al.*, 2008)

1.3 LDH/JOJOBA OIL SUSPENSIONS

Organoclays are rheological modifiers, used as thickeners and for the control of the thixiotropic properties of paints, grease and cosmetics (Jones, 1983). They deliver moderate steady-shear viscosity, together with the formation of a strong gel upon cessation of shear (King *et al.*, 2007). The smectite clay minerals are, however, commonly employed. The thickening of organoclay suspensions is thought primarily to be achieved through exfoliation and/or three-dimensional assemblies of particles into a 'house-of-cards' structure (Albiston, 1996).

However, the delamination of LDH is difficult compared with that of montmorillonites and laponites which exfoliate into single clay sheets in aqueous suspensions (Wu *et al.*, 2005; King *et al.*, 2007). The extent of exfoliation is proportional to the number of delaminated single crystal layers or their small stacks in the matrix. As mentioned earlier, the pristine LDHs are modified with different anions to increase the interlayer distance, consequently improving their propensity to delaminate or exfoliate.

The focus in this section of the study will be mainly on an investigation into the change of viscosity as a function of temperature of organo-LDH/Jojoba oil formulations. As has already been stated, organo-LDHs demonstrate 'thermotropic' behaviour. Therefore the questions are: What effect will the exuded excess acid have on the matrix? Is full exfoliation of organo-LDH in an oil matrix possible? Why Jojoba oil? Jojoba oil (*Simmondsia chinensis*) is a widely used oil phase in cosmetic formulations. The oil has numerous benefits, some of which are improvement of skin tone, excellent oxidative stability and relative stability at high temperatures when compared with other vegetable oils.

1.4 RESEARCH OBJECTIVE

The general objective of the study was to investigate the utility of layered double hydroxides as an additive in polymeric materials and Jojoba oil.

The specific objectives were as follows:

- Extend and optimise the intercalation techniques originally developed for fatty acids and anionic surfactants in hydrotalcite.

- Characterise modified LDH samples by spectroscopic techniques, thermal analysis, X-ray diffraction and microscopy.
- Investigate the properties affected by the incorporation of intercalated clays into candidate polymers, i.e. ethylene vinyl acetate (EVA), ethylene vinyl alcohol (EVAL) and linear low-density polyethylene (LLDPE).
- Prepare and test such nanocomposites, mouldings and oil formulations to confirm suitability for various applications.
- Study the rheological behaviour of organo-LDHs/Jojoba oil suspensions.

1.4.1 Methodology

- Modification of LDHs with long-chain fatty/carboxylic acids which are intended to functionalise the clay and hence improve their compatibility with the matrix
- Comprehensive characterisation of LDHs
- Dispersion of both unmodified and modified LDH through melt compounding, injection moulding of tensile testing dumbbells and mechanical property testing of specimens
- Full characterisation of polymer composites by thermal analysis, and microscopic and spectroscopic studies
- Dispersion of modified LDHs in Jojoba oil, followed by a study of the rheological behaviour of the resultant suspensions.

1.5 REFERENCES

Albiston, L. (1996). Rheology and microstructure of aqueous layered double hydroxide dispersions. *J. Mater. Chem.*, 6(5): 871.

Adachi-Pagano, M., Forano, C. & Besse, J-P. (2000). Delamination of layered double hydroxides by use of surfactants. *Chem. Commun.* : 91–92.

Carlino, S. (1997). The intercalation of carboxylic acids into layered double hydroxides: A critical evaluation and review of the different methods. *Solid State Ionics*, 98, 73–84.

Choy, J-H. (2004). Intercalative route to heterostructured nanohybrids. *J. Phys. Chem. Solids*, 65: 373–383.

Crespo, I., Barriga, C., Rives, V. & Ulibarri, M. A. (1997). Intercalation of iron hexacyano complexes in Zn, Al-hydrotalcite. *Solid State Ionics*, 101–103: 729–735.

Drezdzon, M. A. (1988). Synthesis of isopolymetalate-pillared hydrotalcite via organic-anion-pillared precursors. *Inorg. Chem.*, 27: 4628–4632.

Fischer, H. (2003). Polymer nanocomposites: From fundamental research to specific applications. *Mat. Sci. Eng., C*, 23: 763–772.

Focke, W. W., Nhlapo, N. S., Moyo, L. & Verryn, S. M. C. (2010). Thermal properties of lauric and stearic acid-intercalated layered double hydroxides. *Mol. Cryst. Liq. Cryst.*, 521(1): 168–178.

Jones, R. (1983). The properties and uses of clays which swell in organic solvents. *Clay Min.*, 18(4): 399–410.

Khan, A. & O'Hare, D. (2002). Intercalation chemistry of layered double hydroxides: Recent developments and applications. *J. Mater. Chem.*, 12: 3191–3198.

King, H., Milner, S., Lin, M., Singh, J. & Mason, T. (2007). Structure and rheology of organoclay suspensions. *Phys. Rev. E.*, 75(2): 1–20.

Kumar, A. P., Depan, D., Singh Tomer, N., & Singh, R. P. (2009). Nanoscale particles for polymer degradation and stabilization—Trends and future perspectives. *Progress in Polymer Science*, *34*(6): 479–515.

Leroux, F. & Besse, J.-P. (2001). Polymer interleaved layered double hydroxide: A new emerging class of nanocomposites. *Chem. Mater.*, 13(10): 3507–3515.

Meyn, M., Beneke, K. & Lagaly, G. (1990). Anion-exchange reactions of layered double hydroxides. *Inorg. Chem.*, 29: 5201–5207.

Moyo, L., Focke, W. W., Labuschagne, F. J. & Verryn, S. (2012). Layered double hydroxide intercalated with sodium dodecyl sulphate. *Mol. Cryst. Liq. Cryst.*, 555(1): 51–64.

Newman, S. P. and Jones, W. (1998). Synthesis, characterization and layered double hydroxides containing organic guests. *New J. Chem.*: 105–115.

Nhlapo, N., Motumi, T., Landman, E., Verryn, S. M. C. & Focke, W. W. (2008). Hydrotalcite: Surfactant-assisted fatty acid intercalation of layered double hydroxides. *J. Mater. Sci.*, 43(3): 1033–1043.

Oriakhi, C. O., Farr, I. V. & Lerner, M. M. (1996). Incorporation of poly(acrylic acid), poly(vinylsulphonate) and poly(styrenesulphonate). *J. Mater. Chem.*, 6(1): 103–107.

Reichle, W. T. (1986). Synthesis of anionic clay minerals (mixed metal hydroxides, hydrotalcite). *Solid State Ionics*, 22: 135–141.

Research and Markets. Available at: http://www.researchandmarkets.com [Accessed 11 January 2011].

Robins, D. S. & Dutta P. K. (1996). Examination of fatty acid exchanged layered double hydroxides as supports for photochemical assemblies. *Langmuir*, 12: 402–408.

Utracki, L. A. (2004). *Clay-Containing Polymeric Nanocomposites*, Vol. 1. Shrewsbury, UK: Rapra Technology Ltd, p. 456.

Wu, Q., Olafsen, A., Vistad, Ø. B., Roots, J. & Norby, P. (2005). Delamination and restacking of a layered double hydroxide with nitrate as counter anion. *J. Mater. Chem.*, 15(44): 4695–4700

Xu, Z. P. & Zeng, H. C. (2001). Decomposition pathways of hydrotalcite-like compounds $MgAl_x$ $(OH)_2(NO_3)_x \cdot nH_2O$ as a continuous function of nitrate anions. *Chem. Mater.*, 13: 4555–4563.

Chapter 2

Layered double hydroxides and fatty acid intercalation

Monocarboxylic acids C_{14}–C_{22} were successfully intercalated into Mg-Al-LDH-CO_3. The one-pot synthesis consistently yields a bilayer intercalated product for the range of acids employed. The intercalated anions have an orientation tilt angle of 55–63° depending on the chain length. The thermotropic behaviour of the bilayer fatty acid-intercalated LDHs was studied for each of the fatty acid derivatives within a temperature range of 25–200 °C. The stages followed included removal of water and exudation of excess anions, resulting in a monolayer arrangement.

2 LAYERED DOUBLE HYDROXIDES

2.1 WHAT IS A LAYERED DOUBLE HYDROXIDE?

Layered double hydroxides (LDHs) are also known as hydrotalcite-like compounds. Hydrotalcite was first discovered in Sweden in 1842. The mineral is formed from the weathering of basalts or their precipitation in saline water sources (Braterman *et al*, 2004). Its name derived from its high water content (*hydro*) and talc-like properties, translating to hydrotalcite. The synthetic analogues were first prepared in the laboratory by Feitknecht and Gerber in 1942. They possess a brucite $Mg(OH)_2$ structure in which some of the divalent ions are isomorphously replaced by the trivalent ones. The replacement results in a net positive charge which is counterbalanced by the existence of anions and water molecules in the interlayer. The electrostatic interaction and hydrogen bonding between the layers and the interlayer anions help maintain the overall structure and electro-neutrality of the clay (Cavani *et al.*, 1991; Trifiro & Vaccari, 1996). A schematic presentation of layered double hydroxides is shown in Figure 2.1. LDHs have a generic formula as shown below (Brindley & Kikkawa, 1979; Miyata, 1980; Mascolo & Marino, 1980; Cavani *et al.*, 1991).

$$[M^{2+}_{(1-x)}M^{3+}_{x}(OH)_2]^{x+}(A^{n-})_{(x/n)}\cdot mH_2O$$

where:

M^{2+} is Mg, Zn, Ni, Co, Ca, Mn, etc.

M^{3+} is Al, Cr, Fe, Mn, Co, V, etc.

A^{n-} is CO_3^{2-}, Cl^-, NO_3^-, etc.

The different compositional species derived thereof are referred to as 'hydrotalcite analogues'. In the Mg-Al LDHs, the *x*-value is the ratio of aluminium to magnesium. It is calculated from the equation below:

$$x = \frac{\text{M (III)}}{M(II)+M(III)} \qquad [1]$$

where M(II) and M(III) are the divalent and trivalent cations respectively. The *x*-value is reported to fall within $0.1 \leq x \leq 0.5$, with pure phases existing for $0.2 \leq x \leq 0.3$ (Cavani *et al.*, 1991; Khan & O'Hare, 2002). When the *x*-value is lower than 0.33, the Al octahedrals

are not neighbouring, leading to a high density of Mg octahedrals in the brucite–like sheet. In the case of higher values of *x*, the increased number of neighbouring Al octahedrals leads to the formation of $Al(OH)_3$. The *x*-value determines the layer charge density and the anion exchange capacity (AEC) (Utracki *et al.*, 2007).

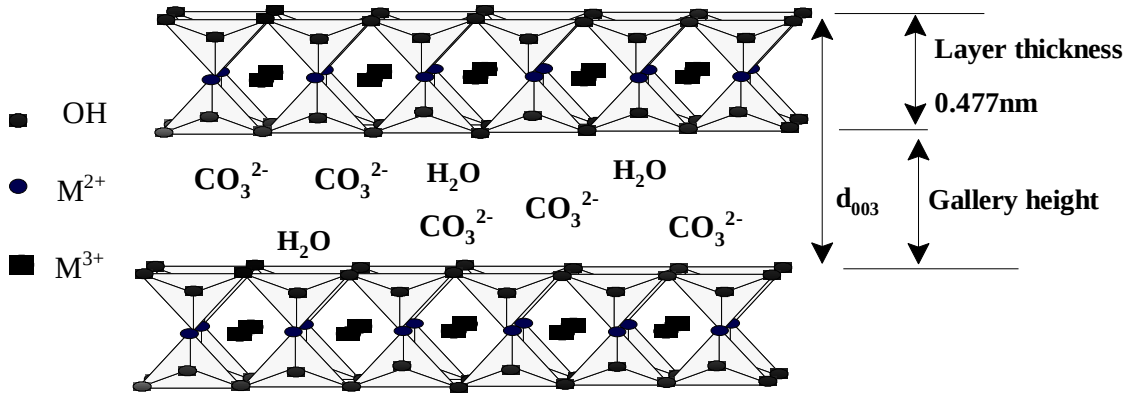

Figure 2.1. Layered structure of LDH-CO_3

The ionic radii of the metal species used in the preparation are usually very close to that of Mg^{2+}. However, when the metal ion radius is above 0.06 nm, the LDH structure becomes unstable, e.g. with cations such as Ca^{2+} the hydrotalcite structure transforms into hydrocalumite (Forano *et al.*, 2006). Several hybrids of LDHs may be synthesised with different stochiometries and metal compositions. Though most research focuses on the binary metal combinations, ternary and quaternary combinations have also been reported (Kooli *et al.*, 1995; Xiang *et al.*, 2009). Hydrotalcite are attractive compared with other layered compounds due to their versatility, ease of tailoring to suit functionality, simplicity and their low cost in preparation. Synthetic analogues of hydrotalcite can be readily prepared in the laboratory.

Hydrotalcite exists as two polymorphs: the hexagonal (H) and rhombohedral (R). The natural varieties of polymorphs have been described as 1H, $2H_1$, $3H_2$, $3R_1$, $3R_2$ and 6R. However, they have been found to occur as a mixture. The most common polytype in synthetic varieties is $3R_1$ (Zaneva & Stanimirova, 2004). The polymorphs are given the above-mentioned designations to describe the stacking sequence of the brucite-like sheets. Table 2.1 is a summary of the different species of layered double hydroxides, polytypes and chemical formulas.

Table 2.1. Summary of layered double hydroxides, year of discovery, polytypes and chemical formulas (Adapted from Zaneva & Stanimirova, 2004)

Year of Discovery	Mineral name	Polytype	Chemical formula
1842	Hydrotalcite	3R	$Mg_6Al_2(OH)_{16}CO_3{\cdot}4H_2O$
1865	Pyroaurite	3R	$Mg_6Fe_2(OH)_{16}CO_3{\cdot}4H_2O$
1866	Woodwardite	3R	$Cu_5Al_2(OH)SO_4{\cdot}2\text{-}4H_2O$
1900	Sjögrenite	2H	$Mg_6Fe_2(OH)_{16}CO_3{\cdot}4H_2O$
1910	Stichtite	3R	$Mg_6Cr_2(OH)_{16}CO_3{\cdot}4H_2O$
1934	Hydrocalumite	2M	$Ca_8Al_4(OH)_{24}(CO_3,Cl,OH)_3{\cdot}11H_2O$
1940	Manasseite	2H	$Mg_6Al_2(OH)_{16}CO_3{\cdot}4H_2O$
1941	Barbertonite	2H	$Mg_6Cr_2(OH)_{16}CO_3{\cdot}4H_2O$
1956	Honessite	3R	$Ni_6Fe_2(OH)_{16}SO_4{\cdot}nH_2O$
1957	Takovite	3R	$Ni_6Al_2(OH)_{16}CO_3{\cdot}4H_2O$
1967	Reevesite	3R	$Ni_6Fe_2(OH)_{16}CO_3{\cdot}4H_2O$
1967	Iowaite	3R	$Mg_5Fe(OH)_{12}Cl{\cdot}2H_2O$
1975	Meixnerite	3R	$Mg_6Al_2(OH)_{16}(OH)_2{\cdot}4H_2O$
1979	Desautelsite	3R	$Mg_6Mn_2(OH)_{16}CO_3{\cdot}4H_2O$
1980	Comblainite	6R	$Ni_6Co_2(OH)_{16}CO_3{\cdot}4H_2O$
1982	Chlormagaluminite	2H	$Mg_4Al_2(OH)_{12}(Cl,CO_3){\cdot}4H_2O$
1992	Caresite	3R	$Fe_4Al_2(OH)_{12}CO_3{\cdot}4H_2O$
1995	Zincowoodwardite	3R	$Zn_5Al_2(OH)_{12}SO_4{\cdot}2\text{-}4H_2O$
1996	Kuzelite	6R	$Ca_4Al_2(OH)_{12}SO_4{\cdot}6H_2O$
1997	Quintinite-2H	2H	$Mg_4Al_2(OH)_{12}CO_3{\cdot}4H_2O$
1997	Quintinite-3T	3R	$Mg_4Al_2(OH)_{12}CO_3{\cdot}4H_2O$
1997	Zaccagnaite	2H	$Zn_4Al_2(OH)_{12}CO_3{\cdot}3H_2O$
1998	Charmarite (2H, 3T)	2H, 3R	$Mn_4Al_2(OH)_{12}CO_3{\cdot}4H_2O$
2000	Woodallite	3R	$Mg_6Cr_2(OH)_{16}Cl_2{\cdot}4H_2O$

2.2 LDH PREPARATION ROUTES

2.2.1 Co-precipitation

Co-precipitation is a direct synthesis method that entails nucleation and growth of metal hydroxide layers from two metal species in a basic aqueous solution. The metal salts favoured in this reaction are nitrates and chlorides. This is due to their monovalent charge

which makes them easily exchangeable. Due to the frequent use of the method in the preparation of LDHs, various refinements have been employed. These include:

- Co-precipitation in aqueous solution (Boclair & Braterman, 1999)
- Co-precipitation in non-aqueous solution (He *et al.*, 2005)
- Hydrothermal synthesis by urea hydrolysis (Rao *et al.*, 2005)
- Co-precipitation at low supersaturation (Meyn *et al.*, 1990)
- Co-precipitation at high supersaturation (Constantino & Pinnavaia, 1995)

During synthesis, researchers pay special attention to the nature and mole ratio of the metal species, nature of anions, pH, temperature, precipitation method and the post-preparation treatment of the LDHs. The method allows control of the charge density of the hydroxide layers by regulating the pH of the system. When the pH of the system is too low, not all the mixed metal ions will precipitate, whereas a very high pH leads to the dissolution of one or more of the ion species (Othman *et al.*, 2009). As the precipitate is often in the form of gels, washing tends to be complicated, resulting in very low yields.

2.2.2 Urea hydrolysis

The methods usually follow the principles of the co-precipitation reaction. However, the base or precipitating agent is generated in situ. The method has been used with much success by many researchers (Adachi-Pagano *et al.*, 2003, Rao *et al.*, 2005, He *et al.*, 2005). Urea is a weak Brønsted base, whose hydrolysis rate is controlled by temperature. Hydrolysis proceeds in a two-step process:

(i) The rate-determining step, which entails the formation of ammonium cyanate:

$$H_2NCONH_2 \rightarrow NH_4^- + NCO^-$$

(ii) Fast hydrolysis of the cyanate into ammonium carbonate:

$$NH_4CNO + 2H_2O \rightarrow (NH_4)_2CO_3$$

The hydrolysis process of ammonium cyanate to ammonia and carbonate to hydrogen carbonate gives a pH of approximately 9, which is ideal for the precipitation of hydroxides. The resulting LDHs show good crystallinity and large particles. Since the reaction

progresses slowly, this leads to low degrees of supersaturation. Temperature control was observed to be a fundamental parameter for obtaining uniformity and particle sizes (Othman *et al.*, 2009). Iyi *et al.* (2004), used an alternative ammonia releasing/precipitating agent in the form of hexamethylenetetramine (HMT) and they were able to achieve high degrees of crystallinity. However, the production of the carbonate anion is unavoidable in all cases. Microwave synthesis of hydrotalcite by urea hydrolysis was employed by Yang *et al.* (2007), and the hydrotalcite prepared at 600 W power had the highest crystallinity and a homogeneous crystal size.

2.2.3 Sol-gel

The sol-gel technique was pioneered by Lopez *et al.* (1996) in the synthesis of hydrotalcite analogues. The sol is prepared by hydrolysis and condensation of the inorganic salt and organic metal compound (alkoxides) in water and/or organic solvent. Variants of the method include heating and using different types of solvent to achieve dissolution of less-soluble reactants (Othman *et al.*, 2009). Ramos *et al.* (1997) prepared hydrotalcites from magnesium ethoxide using various sources of aluminium, i.e. acetylacetone, nitrate, sulphate and chloride. The crystallinity of the product and sintering behaviour was found to depend on the aluminium precursor. The observed properties followed this trend: aluminium acetylcetonate > aluminium chloride > aluminium nitrate > aluminium sulphate.

Prinetto *et al.* (2000) also explored sol-gel techniques in the preparation of hydrotalcite and takovite analogues. The starting materials were metal alkoxides and/or acetylacetonate. This preparation method led to pure and well-dispersed nanomaterials. LDH particles derived in this way have a lower particle size and are more reactive compared with those obtained by the co-precipitation reaction (Jitianu *et al.*, 2003). Samples prepared by this method exhibited an increase in specific surface area, which is attributed to an increase in mesopore volume (Forano *et al.*, 2006). These mesoporous structures are ideal for the development of novel catalysts or catalytic systems. Sol-gel LDH properties have been modified by changing the cations used in the sol preparation, the reaction temperature, the ageing time the pH. For example, decreasing the reaction temperature or ageing time increases the specific surface area or particle size of LDHs. The specific surface area of the LDHs was found to be 10–25% greater than that of products achieved from the co-precipitation reaction (Aramendia *et al.*, 2002). Increasing the acid-boehmite molar ratio was

recommended to decrease the porosity of the sintered LDHs (Othman *et al.*, 2009). The areas of concern in this method include the basicity and their M^{II}:M^{III} ratio.

Other methods that have been employed in the preparation of LDHs include electrochemical methods (Sugimoto *et al.*, 1999; Indira *et al.*, 1994), steam activation (Abello *et al.*, 2006), hydrothermal crystallisation of the amorphous acidic precursor (Mascolo *et al.*, 1995) and *chimie douche* (Delmas & Borthomieu, 1993).

2.2.4 Post-preparation techniques

Post-preparation techniques are carried out to improve the quality of crystallites, obtain uniform size distribution and improve the ordering of anions within the interlayer of the LDH. These post-preparation techniques include hydrothermal and solvothermal methods, microwave irradiation and ultra-sound treatments.

Hydrothermal treatment is the most common of the methods used. The sample is subjected to temperatures of up to 200 °C under autogeneous pressure for time periods ranging from hours to days. This treatment has given rise to increases in particle size relative to the ageing time. The LDH platelets obtained thereof are of regular shapes, usually hexagonal morphologies.

Microwave treatments are normally used in combination with hydrothermal methods. However, the advantages of the former over the latter include shorter reaction time. For example, a well-crystallised product was obtained in 12 minutes compared with 1 530 minutes (Kannan *et al.*, 2000). As microwaves interact with liquid or solid materials, they produce a dipole re-orientation in dielectric material and ionic conduction if the ions are mobile. Hence it is possible to achieve a uniform bulk heating of the system, reducing the occurrence of thermal gradients originating from the conventional heating method (Othman *et al.*, 2009).

It is clear from the above preparation methods that hydrotalcites can be tailored to fit their specific requirements and properties. The high charge density on the LDHs renders them unattractive as they do not readily exfoliate or delaminate. LDHs possess an expandable 2-D layer structure which allows the exchange of various anions. Increasing the d-spacing

lowers the van der Waals force between the sheets, hence they can easily be exfoliated or delaminated. Expansion of the interlayer is achieved by a process called *intercalation*.

2.2.5 Texture and morphology

The texture and morphology of platelets are related to the preparation method and crystal growth habits. Like most clay materials, LDHs exhibit a layered structure. Crystal habits similar to those observed in smectite single crystallites are also observed in LDHs, i.e. laths, fibres, and subhedral and euhedral lamellae (see Figure 2.1). The hexagonal shape obtained mainly from the urea hydrolysis method (Yang *et al.*, 2007) has become the archetype of well-synthesised LDHs. The hexagonal and rhombohedral shapes fall into the euhedral lamellae category. They display the presence of well-developed {*hk0*} in addition to a very prominent basal reflection (Grim & Güven, 1978). This is typical of crystals that have had ample space for growth. The majority of researchers observed subhedral forms (Nhlapo *et al.*, 2008, Xu and Braterman 2010, Costa *et al.*, 2006); these have irregular outlines, but with a well-defined basal form. Although the lath and fibre forms are rare, they have been reported (Xu & Braterman, 2010, Moyo et al, 2012). Crystallites of this form originate from the folding of thin lamellae (Grim & Güven, 1978). SEM micrographs of the different LDH crystallites observed in this study are shown in a Section 2.6.1 and Appendix B.

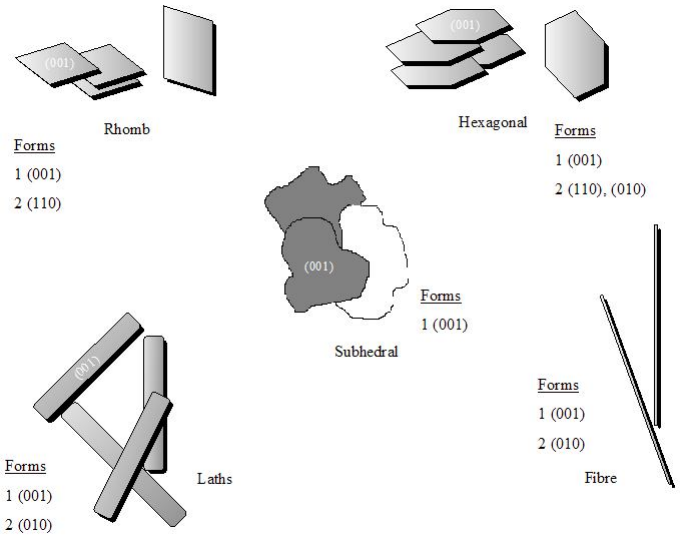

Figure 2.2. Common habits of smectite single crystallites
(Adapted from Grim & Güven, 1978)

2.3 INTERCALATION

Intercalation is a form of clay-surface interaction where the anions or surfactant molecules aggregate within the interlayer, i.e. between pairs of adjacent clay sheets (Crepaldi *et al.*, 2002). O'Hare (1991) defined it as "the reversible insertion of mobile guest species into a crystalline layered host lattice, during which the structural integrity of the latter is formally conserved". Self-assembly drives intercalation. During this process the anions spontaneously organise themselves into an ordered state (see Figure 2.3). The basic mechanism by which intercalation occurs is either through oxidation-reduction, ion-exchange, acid-base or donor-acceptor reactions (Khan & O'Hare, 2002). LDHs are normally non-selective, although shape and stereo-selectivity have been observed (Ikeda *et al.*, 1984; Lotsch *et al.*, 2001). Most recently, chain length selectivity has been encountered in surfactant-mediated exchange of short chain fatty acids, in which the surfactant chain is intercalated preferentially (Moyo *et al.*, 2008). Intercalation is facilitated by interactions such as electrostatic attractions, hydrogen bonding and hydrophobic associations (Whitesides *et al.*, 1991). The separation of the layers is governed by the dimensions and functional group of the anions to be intercalated. Other factors include the AEC level of the anions intercalated, size, orientation and interaction with the hydroxyl lattice (Cavani *et al.*, 1991). The inclusion of organic anions within the interlayer of LDHs is essential to their physical or chemical functionality. Intercalation has been used to change the chemical, electronic, optical and magnetic properties of the host lattice (Khan & O'Hare, 2002).

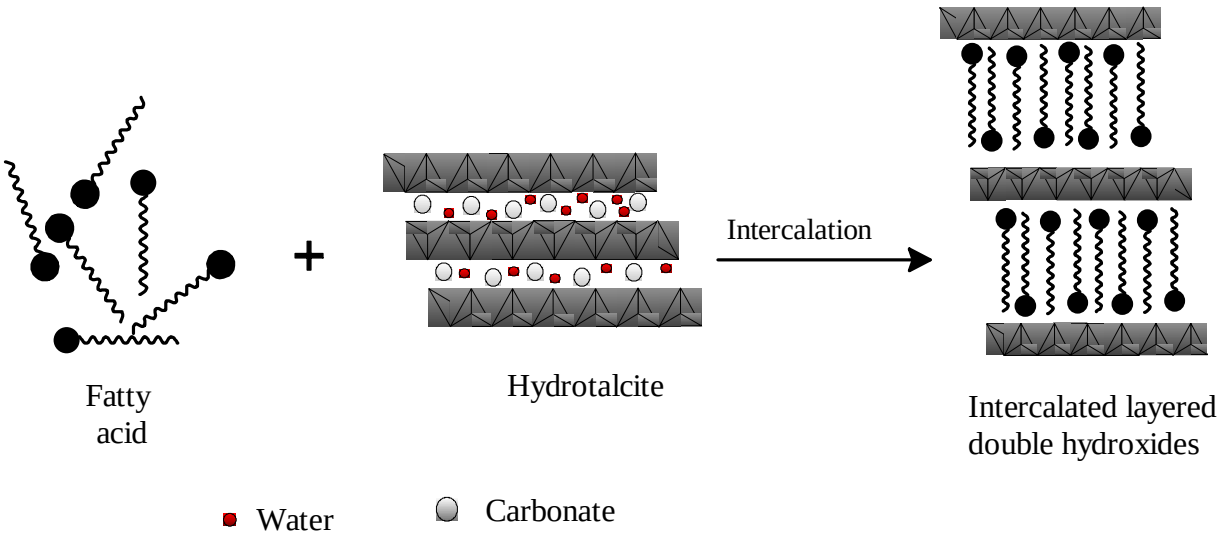

Figure 2.3. Intercalation

2.3.1 Intercalation methods

Crepaldi *et al.* (1999) proposed three main LDH intercalation procedures, i.e. direct synthesis, ion exchange and the regeneration or reconstruction method. Direct synthesis is normally achieved by a co-precipitation reaction (Meyn *et al.*, 1990). The LDH is prepared in situ by adding a mixed metal solution dropwise to an alkaline solution containing the anion to be intercalated. The method has been proved to produce highly crystalline products, especially when followed up by hydrothermal treatments. Moyo *et al.* (2012) employed co-precipitation in the intercalation of dodecyl sulphate, and obtained a pure and highly crystalline bilayer intercalated product.

In the case where the LDH-CO_3 is the precursor, the first step is to eliminate the carbonate anion; this is achieved by either calcination or acid treatment of the LDH-CO_3 (Iyi *et al.*, 2005; Moyo *et al.*, 2008). Hydrotalcite sheets have a high charge density and as a result a higher affinity for multivalent anions such as carbonates. The carbonate anion is therefore tenaciously held within the interlayer. However, the decarbonation process using mineral acids is a challenge due to the strong acidity of HCl and the low acid tolerance of Mg-Al LDH (Iyi *et al.*, 2005).

The LDH precursor in the ion-exchange method is an LDH-A, where A is a monovalent anion that can be easily exchanged, e.g. chloride or nitrate. Miyata and Okada (1977) found that the ease of exchange or affinity of the LDH lattice was found to be in the following order:

$$CO_3^{2-} >> SO_4^{2-} \text{ and}$$

$$OH > F > Cl > Br > NO_3^- > I$$

The LDH-A is suspended in a solution containing the carboxylic acid or its sodium salt. This method has been employed in the intercalation of α,ω dicarboxylic acids and a range of carboxylic acids (Miyata & Kumura, 1973). Variations of the method have included intercalation of lauric, myristic and palmitic acid carried out in ethanolic solutions (Borja & Dutta, 1992).

The reconstruction method is self-explanatory in that the metal hydroxide is reconstructed from the mixed metal oxides. The carbonate anion is removed from the interlayer by heating the LDH-CO_3 at temperatures between 450–550 °C for 3–4 hours. Calcination yields a decarbonised and dehydroxylated layered double oxide (LDO). The LDO is suspended in an alkaline solution containing the anion to be intercalated. The metal hydroxyl lattice reforms under these conditions, at the same time incorporating the anion into the interlayer. The mechanism has been reported to entail a fast rehydration with the intercalation of OH^- anions, which is followed by a slow ion-exchange reaction of the OH^- anions with the desired intercalant (Crepaldi *et al.*, 2002). This is attributed to the memory effect of LDOs. Structure recovery is affected by the calcination conditions, such as temperature, heating rate and duration (Rocha *et al.*, 1999). The method has been used with great success in the intercalation of alkyl-sulphates, aryl sulphonates and carboxylic acids (Miyata & Okada, 1977; Sato *et al.*, 1988; Chibwe & Jones, 1989). Latterini *et al.* (2002) also successfully intercalated large organic anions such as phenolphthalein. Although the method is considered effective, it produces a non-homogeneous product, comprising a mixture of modified LDH and a small fraction of unmodified LDH (Costa *et al.*, 2011). The calcination process can cause irreversible changes in the crystalline structure (Hibino & Tsunashima, 1988; Stanimirova *et al.*, 2001). The texture and morphology of the intercalates was also found to be affected by the calcination process (Moyo, 2009).

The preparation method employed in this particular study of carboxylic acid intercalated LDHs is basically an ion-exchange reaction. However, it is unique in that the exchange is direct from the LDH-carbonate precursor. The underlying principle for the success of the method is a basic acid-base reaction. Carbonic acid has pKa values of 6.35 and 10.33 at 25 °C for the first and second protonation reactions respectively, whereas the pKa value of fatty acids is approximately 4.8. This implies that the fatty acid would readily protonate the carbonate anion (McMurry, 1999; Landman, 2005). This is similar to the decarbonation method described by Iyi *et al.* (2005). They suggested a two-step mechanism by which intercalation occurs, the first step being the protonation of the carbonate anion to hydrogen carbonate and the second step involving the instantaneous inclusion of the anions in solution. However, the method utilised strong acids such as HCl. Limited success was achieved due to the low acid tolerance of Mg-Al LDH and difficulty in handling the acid in large-scale experiments. The method was later modified by using an acetate buffer (sodium acetate buffer and acetic acid/NaCl mixed solution) (Iyi & Sasaki 2008).

Post-intercalative treatments are necessary to obtain a highly crystalline well-ordered product with large particle sizes. These include hydrothermal, microwave and ultra-sound treatments, which have been discussed in greater detail in Section 2.2.4.

2.3.2 Orientation of intercalated fatty acids

Intercalated anions will always orient themselves in such a manner that they maximise interaction with the hydroxyl layers and adjacent anions. The orientation of intercalated anions is studied by X-ray diffraction (XRD) and the state of anions is investigated through Fourier transform infrared (FTIR) spectroscopy. XRD gives an indication of layer separation and FTIR is used to probe the structure of the interlayer and the phase state of intercalated anions. Changes in the CH_2 stretching and scissoring vibrations are related to interlayer packing density, chain length and temperature (Vaia *et al.*, 1994). These aspects are discussed in Section 2.6 (results) of this chapter. Table 2.2. provides a brief overview of orientation and basal spacing of the fatty acid-intercalated LDHs found in the literature.

Table 2.2. Orientation and d-spacing of fatty acid-intercalated LDHs

Intercalated anion	LDH	M^{2+}/M^{3+} ratio	Orientation	d-spacing (nm)	Reference
Myristate	Li-Al; Mg-Al	1:2; 3:1	Monolayer	2.64	Borja & Dutta, 1992
Palmitate	Mg-Al	2:1	Bilayer	4.79	Itoh *et al.*, 2003
	Mg-Al	2:1	Monolayer	2.82	Nyambo *et al.*, 2009
	Zn-Al	2:1	Bilayer	4.42	Xu & Braterman, 2010
Stearate	Mg-Al	3:1	Monolayer	3.16	Meyn *et al.*, 1990
	Mg-Al	2:1	Bilayer	5.37	Itoh *et al.*, 2003
	Mg-Al	2:1	Bilayer	5.04	Nhlapo *et al.*, 2008
	Mg-Al	2:1; 3:1	Monolayer	2.95; 2.82	Xu & Braterman, 2010
	Zn-Al	2:1; 3:1	Bilayer	5.00; 4.99	Xu & Braterman, 2010
Arachidate	Mg-Al	2:1	Bilayer	5.72	Itoh *et al.*, 2003

Generally, two types of orientation have been observed for fatty acid intercalated LDHs, i.e. a monolayer and bilayer, the former being the most common (Figure 2.4). The packing and orientation of carboxylic acids is driven by:

(i) the advanced hydrophobic interaction of long-chain aliphatic carboxylates that intercalate greater-than-normal AEC levels and pack closely in a bilayer format (Itoh *et al.*, 2003)

(ii) molecular packing, which is dependent on the use of excess fatty acids and intercalation temperature (Itoh *et al.*, 2003; Nhlapo *et al.*, 2008)

(iii) the solution pH at which anion-exchange takes place (Kuehn & Poellmann, 2010).

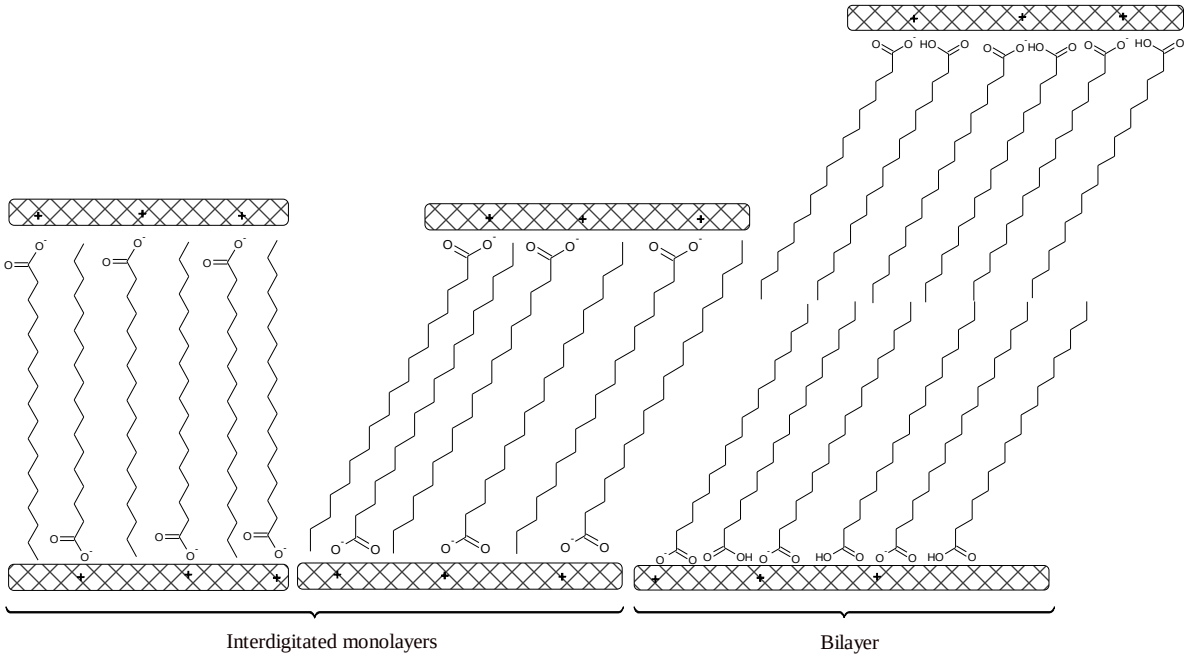

Figure 2.4. Orientation of intercalated fatty acids

Kanoh *et al.* (1991) suggested that LDHs could intercalate fatty acids greater than their normal AEC through the formation of bilayer structures similar to the Langmuir-Blödgett films. The strength, elasticity and stability of an absorbed surfactant film are influenced by surface activity, chain length compatibility and cohesion. Moreover, interactions between polar groups of the molecules in the monolayer have additional influence. The monolayer film of saturated fatty acids compresses to the same limiting area, e.g. stearic acid has a limiting area of 21 Å (Kanicky & Shah 2002; Itoh *et al.*, 2003). Close chain packing is also driven by the length of the surfactant chain (Figure 2.5). The van der Waals interaction between chains increases with increase in the chain length. Hence long-chain surfactants will pack closely and readily as compared with the short-chain carboxylates. This would explain the difficulty encountered by researchers in intercalating chains lengths of C_1 to C_8 (Costa *et al.*, 2011; Nhlapo *et al.*, 2008).

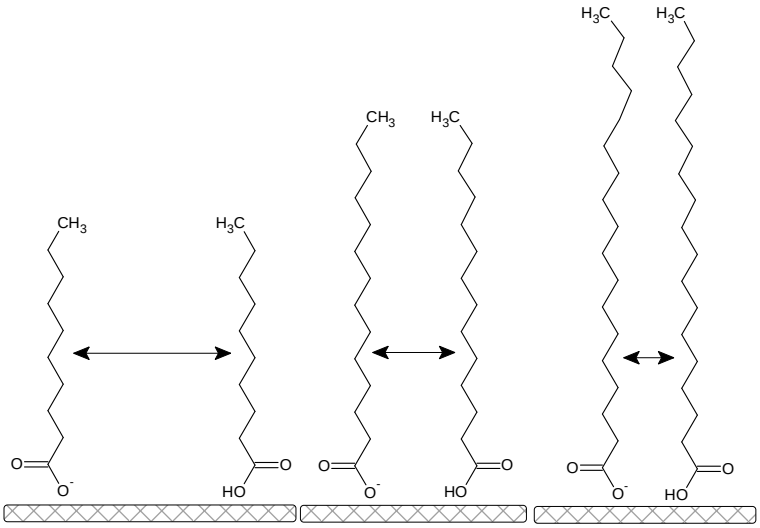

Figure 2.5. Effect of chain length on the close packing of intercalated fatty acids (Adapted from Kanicky & Shah, 2002)

Intercalation is pH dependent: at high pH the surfactant head groups are completely ionised (Figure 2.6). This results in the repulsion of similarly charged molecules, which ultimately leads to expansion of the monolayer and a weak, unstable film. Close packing is achieved when intercalation is carried out close to its pKa value, as seen from Figure 2.6.

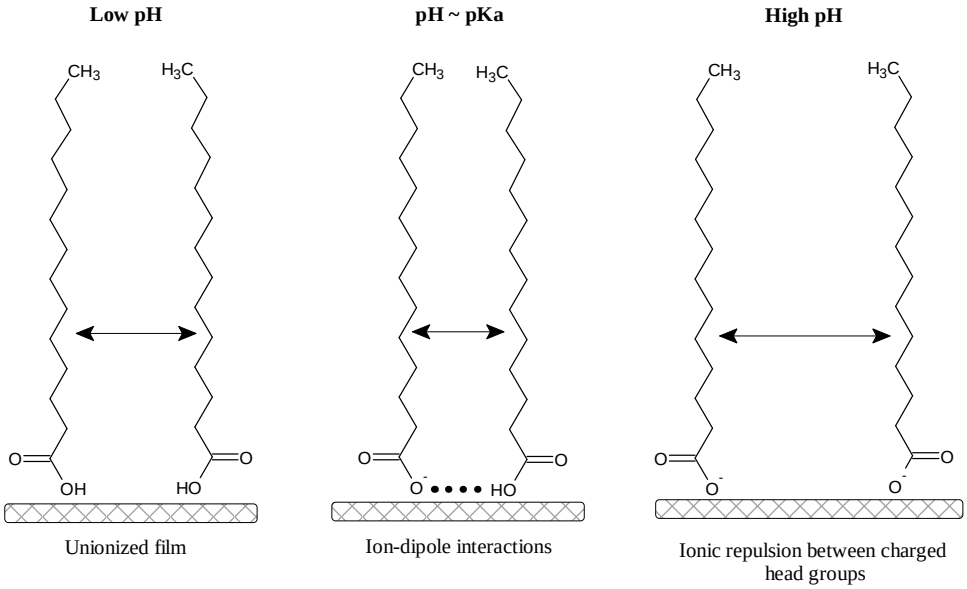

Figure 2.6. Effect of pH on the close packing intercalated fatty acid (Adapted from Kanicky & Shah, 2002)

2.4 CHARACTERISATION OF LDH AND MODIFIED DERIVATIVES

A combination of characterisation techniques is employed in the structural elucidation of LDH, its composition and the orientation of intercalated anions. The most common techniques are powder XRD, FTIR, thermogravimetry (TG), scanning electron microscopy (SEM) and transmission electron microscopy (TEM).

XRD is the main technique used in determining the extent of intercalation through changes in the d-spacing. It is also used to determine the degree of crystallinity, which is a direct function of the organisation within the hydroxide layer. FTIR provides information on the organic species that has been intercalated and the vibrational spectroscopy of the LDH octahedral lattice and hydroxyl groups. Thermogravimetric methods are essential in studying the thermal stability/behaviour of pristine LDHs and their intercalated derivatives. These methods also allow a comprehensive study of the decomposition pathways of LDHs. SEM and TEM are used to study the different textures and morphologies exhibited by LDHs. In addition, they give an appreciation of the lateral dimensions of the LDH platelets.

The other characterisation techniques used in the study are differential scanning calorimetry (DSC), TG-FTIR, temperature scan XRD and FTIR, and inductively coupled plasma optical emission (ICP-OES) spectrometry.

In this phase of the project the aim was to intercalate straight-chain carboxylic acids from C_{14}–C_{22} and fully characterise the organo-LDH obtained thereof.

2.5 EXPERIMENTAL

2.5.1 Materials

The layered double hydroxide LDH-CO_3 (hydrotalcite grade HT-5) was supplied by Nkomazi Chemicals, South Africa. The particle size of the LDH was determined in a Malvern Mastersizer 2000 instrument and the particle size distribution was found to be d(0.1): 1.19 µm; d(0.5): 3.94 µm and d(0.9): 23.93 µm. Various fatty acids were used in the intercalation reactions; their properties are summarised in Table 2.3. They were all saturated

fatty acids (C_{14}–C_{18}), with the exception of oleic acid and Jojoba oil. Jojoba oil is composed of unsaturated liquid wax esters ranging from C_{36}–C_{42}.

Table 2.3. Summary of fatty acids used in the intercalation process

Acid	IUPAC name	Formula	Molar mass	Melting point (°C)	Supplier	Purity
Myristic	Tetradecanoic	$C_{13}H_{27}COOH$	228.37	54	Merck	≥ 98%
Palmitic	Hexadecanoic	$C_{15}H_{31}COOH$	256.42	63	Sigma	≈ 95%
Stearic	Octadecanoic	$C_{17}H_{35}COOH$	284.48	70	Biozone Chemicals	-
Behenic	Docosanoic	$C_{21}H_{43}COOH$	340.58	80	Fluka	≥ 80%
Oleic	(9z)-Octadec-9-enoic	$C_{17}H_{32}COOH$	282.46	14	Merck	

2.5.2 Preparation of organo-LDH

The Mg-Al-LDH-stearate was prepared as reported by Nhlapo *et al.* (2008). A typical intercalation procedure was carried out as follows: 40 g of surfactant (Tween 60) was dissolved in 1.5 litres of preheated distilled water and the temperature was kept at 80 ˚C. The addition of excess stearic acid (0.384 mol which is an equivalent of four times the AEC) was added in a three-part series. The total amount of 109g was added. The mixture was heated at 80 ˚C for 8 h and cooled overnight at room temperature. The process was repeated over four days with continuous stirring. On the fourth the day there was no acid addition. The pH of the mixture was maintained by adding ammonia solution, with each correction carried out once each day and corrected to a pH of approximately 9–10. The mixture was allowed to cool and the solids were separated by centrifugation, washing the mixture four times with water and once each with ethanol and acetone respectively. The LDH-stearate solids were dried at room temperature. The other fatty acids, namely myristic, palmitic and behenic acids, were intercalated in a similar manner. Detailed experimental parameters are documented in Appendix B.

The above procedure was repeated using the exact AEC and twice the AEC. The products were labelled LDH-stearate 1AEC and 2AEC respectively. Another experiment was carried out without stearic acid; this was done to determine whether the Tween 60 could intercalate into the LDH-CO_3 on its own. In addition, the neat magnesium stearate and aluminium stearate were subjected to a similar procedure, but in the absence of the LDH-CO_3.

Re-crystallisation of the magnesium stearate (20 g Mg stearate + 40 g surfactant (Tween 60)) was carried out by suspending it in distilled water. The reaction temperature was adjusted to 80 °C with pH ≈ 9-10 and it was left to run for 24 h. The samples were recovered by centrifugation, washed once with water, three times with ethanol and once with acetone.

A 2:1 molar mixture of magnesium stearate and aluminium stearate was reacted using a very similar process. A mixture of 40 g of Tween 60, 28.38 g (0.048 mol) of magnesium distearate and 21.06 g (0.024 mol) of aluminium tristearate was suspended in 1 000 ml of distilled water and heated to 70 °C. As before, NH_4OH was added to control the pH (pH = 10). The product was recovered as described above. This product was named magnesium/aluminium stearate.

Finally, LDH-oleate was synthesised by the co-precipitation method. Solutions (0.5 and 0.25 mol respectively) of $Mg(NO_3)_2 \cdot 6H_2O$ and $Al(NO_3)_3 \cdot 9H_2O$ were prepared. The mixture of the metal salts solution was added dropwise to an alkaline solution containing 0.35 mol of oleate anions. The pH was adjusted using 2M NaOH to a pH of 10. The temperature was controlled at 80 °C and the solution left to stir for three days. Solids were again recovered by centrifugation and washed with distilled water – four times with ethanol and once with acetone. The solids were oven dried at 60 °C.

2.5.3 Characterisation

ICP-OES was used to determine the elemental composition of the fatty acid-intercalated LDH. Five milligrams of LDH and fatty acid-intercalated LDH samples were leached in an *aqua regia* solution. The aliquots were left to cool; 1 ml of aliquot was diluted with 9 ml of de-ionised water. These were then analysed on a Perkin Elmer SPECTRO ARCOS ICP-OES spectrometer to quantify the amount of Mg and Al present. Calibration was carried out using a multi-element standard (ICP grade). Each sample was measured three times and the average ICP value was recorded.

Powder samples were viewed on a JEOL 5400 SEM and a JEOL JSM-6010LA analytical SEM. They were prepared as follows: a small quantity of the LDH-fatty acid and the LDH-CO_3 precursor was placed onto carbon tape on a metal sample holder. Excess powder was

removed using a single blast of compressed air. The samples were then coated three times with gold under argon gas using the SEM autocoating unit E5200 (Polaron Equipment Ltd). Elemental analysis of the LDHs was done on the JEOL 5400SEM with Energy-dispersive X-ray spectroscopy (EDS). Transmission electron microscopy (TEM) was carried out on a JEOL 2100 TEM. A small quantity of LDH-CO_3 was added to 5 ml of methanol. A homogeneous dispersion was obtained through sonication for 5 to 10 s. Drops of the colloidal liquid were placed on an Agar scientific 300 µm holey carbon film coated copper grid. The solution was allowed to dry out prior analysis.

Phase identification was carried out by XRD analysis on a PANalytical X-pert Pro powder diffractometer with variable divergence and receiving slits and an X'celerator detector using Fe-filtered Co K-alpha radiation (0.17901 nm). X'Pert High Score Plus software was used for phase identification. Temperature-resolved XRD traces were obtained using an Anton Paar HTK 16 heating chamber with a Pt heating strip. Scans were measured between 2θ = 1° to 40° in a temperature range of 25 to 200 °C in intervals of 10 °C with a waiting time of 1 min and measurement time of 6 min per scan. Si (Aldrich 99% pure) was added to the samples so that the data could be corrected for sample displacement using X'Pert High Score plus software.

Differential scanning calorimetry (DSC) data were collected on a Perkin Elmer DSC instrument. Samples of 5–10 mg were placed in a 40 µl alumina pan and heated from -40 to 200 °C and then cooled back to -40 °C at a scan rate of 5 °C/min and a N_2 flow rate of 50 ml/min.

Thermogravimetric analysis was carried out on the neat LDH-CO_3 and the fatty acid-intercalated LDH. A powder sample of 15 mg was analysed on a Mettler Toledo TGA A851 TGA/SDTA machine. The sample was placed in 70 µl alumina open pans. The temperature was scanned at 10 °C/min in air, ranging from 25 to 1 200 ^{o}C.

Standard FTIR was carried out on a Perkin Elmer 100 Spectrophotometer with a MIRacle ATR attachment with diamond Zn/Se plate; spectra were recorded between 4000 and 650 cm^{-1} at a resolution of 2 cm^{-1}, and the data collected over 32 scans.

2.6 RESULTS AND DISCUSSION

2.6.1 Composition and morphology

The ICP data are reported as mol ratio relative to aluminium (Table 2.4). The LDH-CO_3 precursor used in the study is represented by the formula $[Mg_{1-x}Al_x(OH)_2](CO_3)_{x/2}\cdot nH_2O$, where *x* quantifies the fractional replacement of Mg by Al ions in the hydroxide sheets. Several studies have cited the tendency of fatty acids to co-intercalate with their sodium salts (Kanoh *et al.*, 1999; Itoh *et al.*, 2003; Nhlapo *et al.*, 2008). To cater for this scenario the general formula for the intercalated LDH was $[Mg_{1-x}Al_x(OH)_2]\{(CHO)_x(NaCHO)_y\}\cdot nH_2O$.

Table 2.4. Compositional data and formulae for the LDH-CO_3 precursor and intercalated products

LDH	Aluminium mol ratio to		
	Mg	**Na**	***x***
Carbonate	2.33	0.14	0.30
Myristate	1.92	0.04	0.34
Palmitate	2.39	0.02	0.30
Stearate	1.98	0.03	0.34
Behenate	1.95	0.02	0.34

Pristine LDH-CO_3 has a sand-rose morphology when viewed under the SEM. Several researchers have described the morphology of pristine LDH particles as having a plate-like hexagonal shape (Yang *et al.*, 2007). However, their form is not well defined as viewed in the micrographs below. It is composed of very small subhedral platelets with a lateral average size of 1–5 µm. The particle size distribution will differ from one synthesis method to another (Costa *et al.*, 2008). The same morphology can be observed from both SEM (Figure 2.7a) and TEM Figure 2.7b, c & d. In the case of an LDH-platelet placed on edge, the different stratification of the layers can be observed (Figure 2.7d).

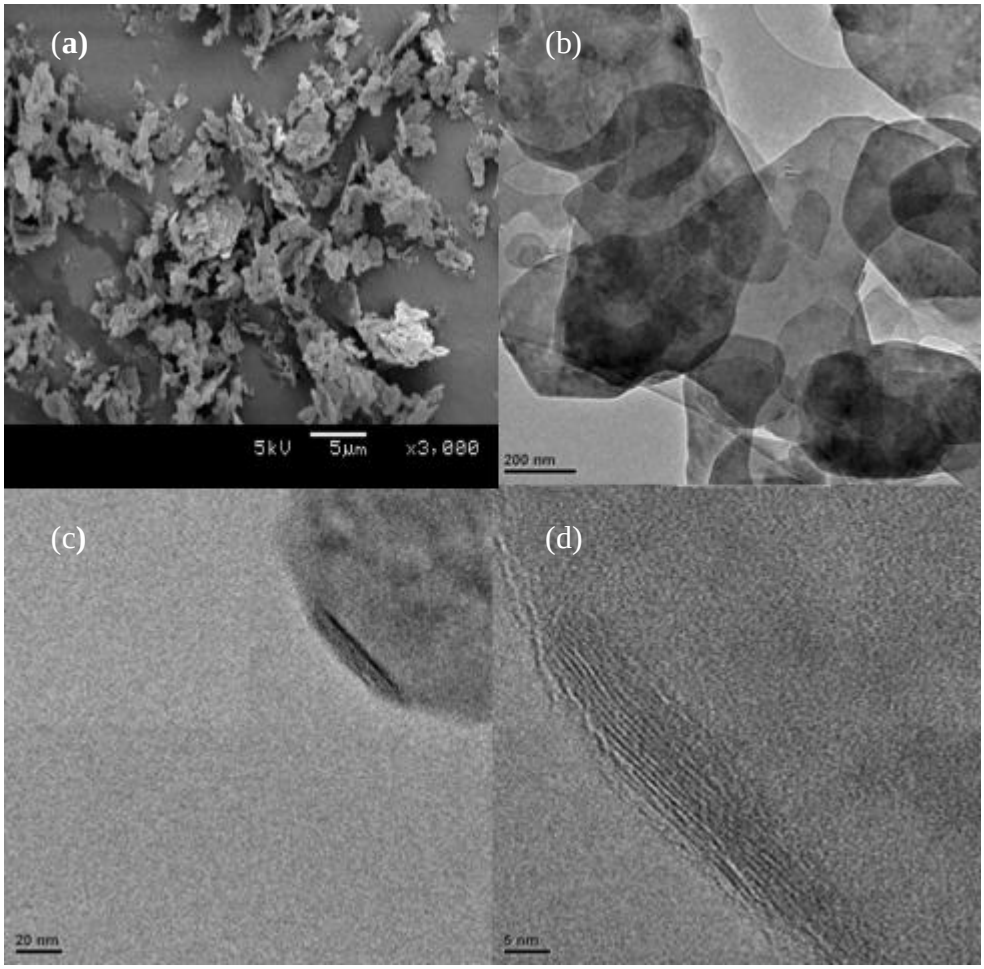

Figure 2.7. (a) SEM; (b), (c) and (d) TEM micrographs of neat LDH-CO_3

The modified LDH appears to have larger platelets (Figure 2.8). This suggests that the modification process involves dissolution and recrystallisation of the parent LDH to the organo-LDH (Cavani *et al.*, 1991). The organo-LDHs generally exhibited irregular subhedral shapes, with the exception of the LDH-palmitate which showed distinct euhedral platelets with a rhombohedral shape.

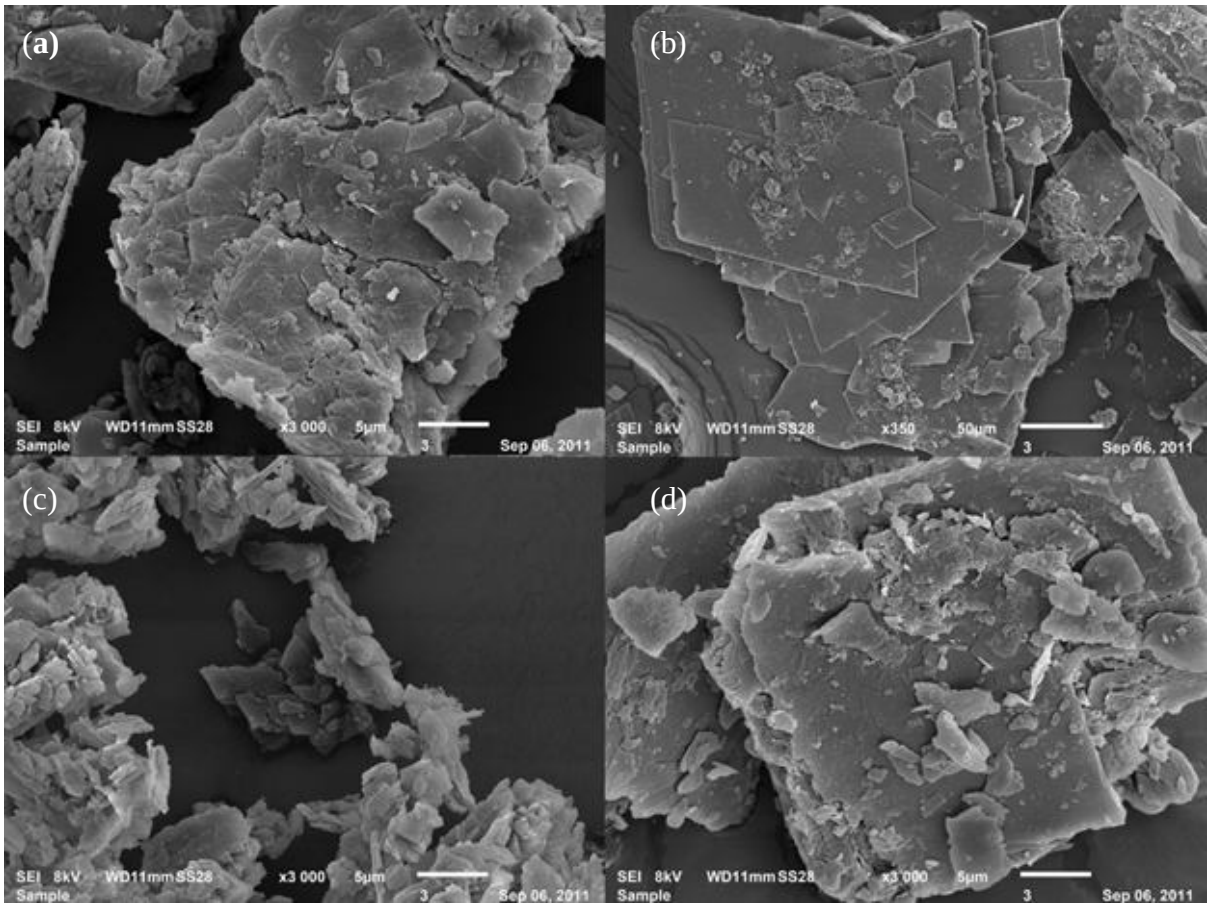

Figure 2.8. SEM micrographs of the LDH samples: (a) LDH-myristate; (b) LDH-palmitate; (c) LDH-stearate; and (d) LDH-behenate

The composition of the platelets was probed by energy dispersive X-ray spectroscopy (EDS). The ratio of Mg to Al is similar or very close to those reported in ICP results. However, it is interesting to note that the well-defined rhombohedral-shaped platelets showed varying Mg:Al ratios. Figures 2.9(a) & (b) shows a typical example with a variety of compositions obtained in LDH-palmitate platelets. The EDS data of the other fatty acid-LDH derivatives are given in Appendix B. This could be an indication that the intercalation process used in the study is followed by dissolution and recrystallisation of the LDH lattice. This is similar to the findings of Grover *et al.* (2010), who explained the changes in the morphology of arsenic-intercalated LDH and hydrocalumite in terms of the anion-exchange mechanism which occurs via a dissolution–precipitation reaction.

(a)

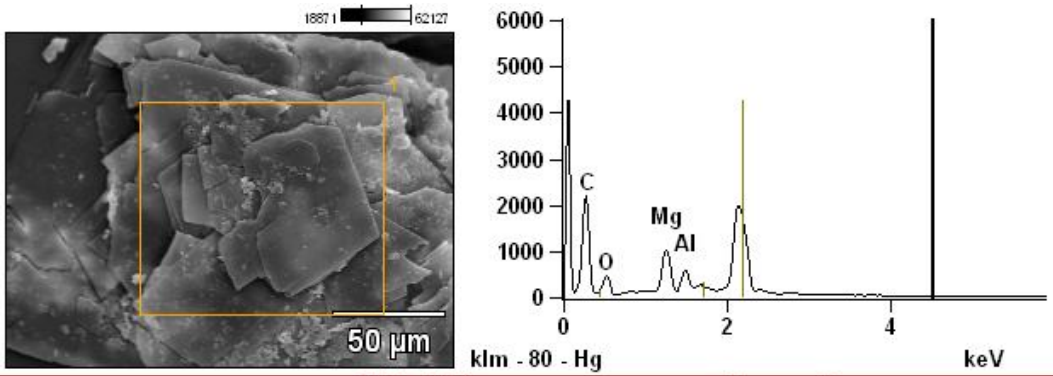

	Weight %		Atom ratio		
	Mg	Al	Mg	Al	Mg/Al ratio
LDH-palmitate_pt1	31.2	16.8	1.3	0.62	2.09

Weight % Error (+/- 1 Sigma)

	Mg	Al
LDH-palmitate_pt1	+/-0.6	+/-0.7

(b)

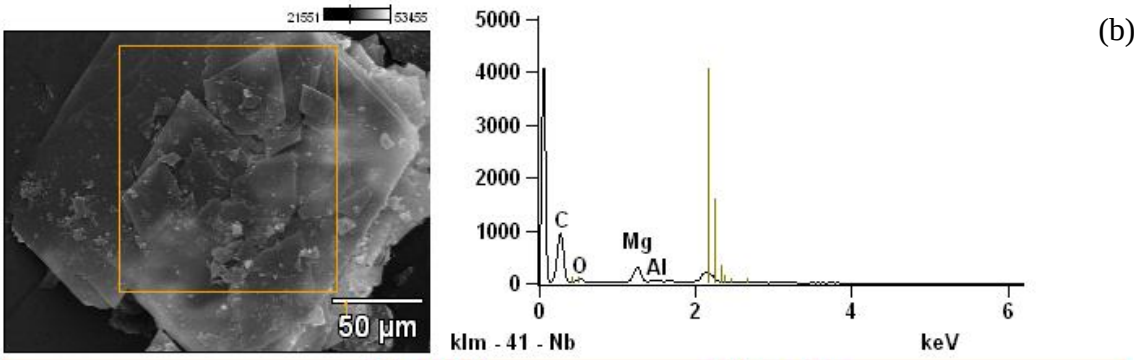

	Weight %		Atom ratio		
	Mg	Al	Mg	Al	Mg/Al ratio
LDH-palmitate_pt1	41.4	6.7	1.73	0.25	6.95

Weight % Error (+/- 1 Sigma)

	Mg	Al
LDH-palmitate_pt1	+/-1.1	+/-0.8

Figure 2.9. EDS data showing different compositions of LDH-palmitate platelets with Mg:Al ratios of (a) 2.09 and (b) 6.95

The elemental analysis by EDS indicates the existence of Mg and Al, with their atomic composition ranging from 1.65 to 6. However, some of the platelets were composed of only Mg; the data on this sample is shown in Appendix B. Zhang *et al.* (2012) also found that increasing concentrations of sodium dodecyl sulphate (SDS) during intercalation resulted in

the product changing from CaAl-SDS to Ca-SDS. The interlayer spacing increased from 2.72 to 3.25 nm.

2.6.2 X-ray diffraction analysis

The morphology, particle size and crystallinity of LDHs are directly related to the organisation of the metal hydroxide lattice. Reaction parameters such as preparation time, temperature, concentrations of reactants, post-preparation treatments and reaction solvents all contribute to these properties (Braterman *et al.*, 2004). Broad powder XRD peaks are normally assigned to phases that lack order, while the narrow sharp peaks are indicative of well-ordered and crystalline phases. A high degree of crystallinity is indicated by the presence of well-resolved XRD patterns (Forano *et al.*, 2006). XRD may also be used as an indicator of phase purity.

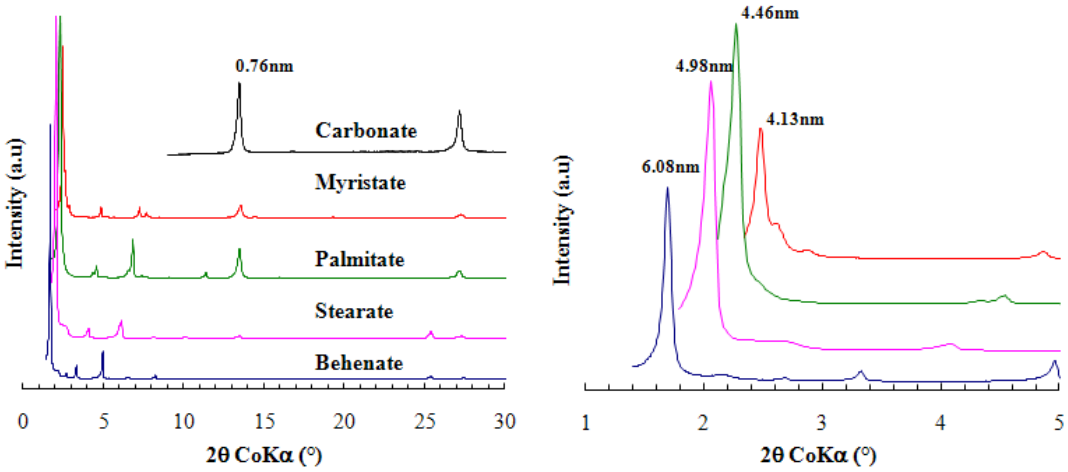

Figure 2.10. WAXS diffractograms of the neat and modified LDH

Assuming the LDH has a rhombohedral stacking order, the basal reflections may be indexed as 003, 006, etc. (Braterman *et al.*, 2004). The characteristic peaks of LDH-CO_3 are observed at 2θ values of 13.5 and 27.2°. These 2θ values are typical for LDH-CO_3, with a d-spacing (d_L) of 0.76 nm. A shift to lower 2θ values is an indication of layer separation or an increase in d-spacing. All the fatty acid-intercalated LDHs showed an increase in the d-spacing; these were observed to be 4.13, 4.46, 4.98 and 6.08 nm for the myristate, palmitate, stearate and behenate respectively (see Figure 2.10). The peak positions are consistent with a bilayer orientation of fatty acid ions. The d-spacing increases linearly with the increase in the number of carbon atoms of the carboxylic acids, as shown in Figure 2.11.

The intercalated fatty acid anions are envisaged to have a tilt angle of 56–59°, basing the calculation on the equation given below (Carlino, 1997; Xu & Braterman, 2010).

$$d = 1.48 + 0.26(n - 2)\sin\theta \qquad [2]$$

where

d is the d-spacing

n is the carbon number in the stearate chain

θ is the slant angle of the intercalated fatty acid anions.

The data obtained experimentally fit well with the theoretical calculation and those obtained from other studies, as seen in Table 2.2. Trace LDH-carbonate phases were present, particularly in the myristate and palmitate. The peaks are sharp and symmetric, which is an indication of good ordering in the synthesised intercalates.

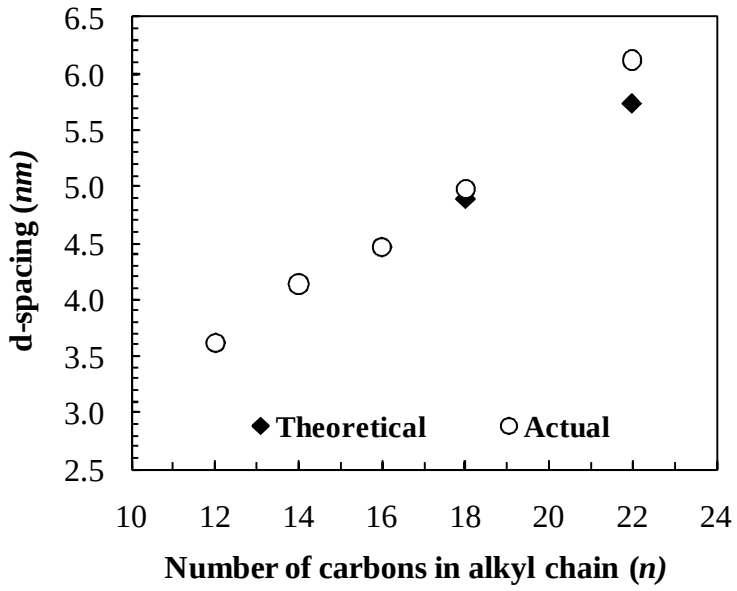

Figure 2.11. Increase in basal spacing with increase in alkyl chain lengths (○) obtained experimentally in this study and (♦) obtained from theoretical calculations

2.6.3 Fourier transform infrared analysis (FTIR)

This technique helps to identify the type of intercalated species and their state within the interlayer.

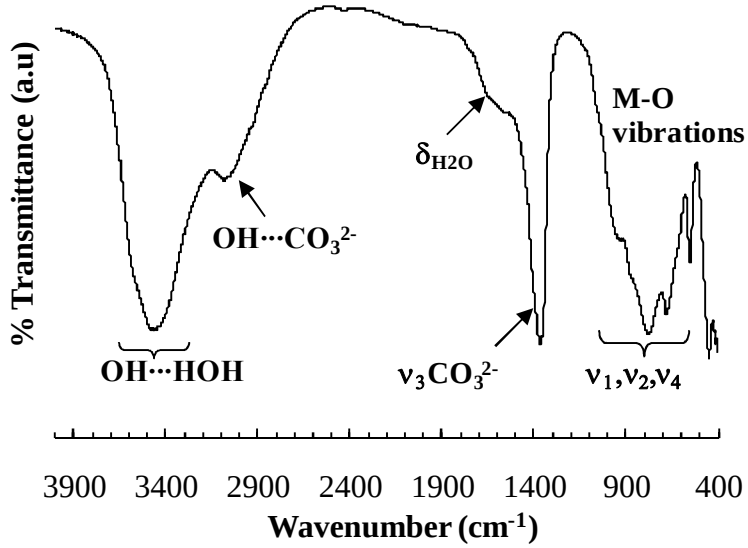

Figure 2.12. Pristine LDH and its typical FTIR vibrations

Figure 2.12 shows FTIR peaks that are typical for the pristine LDH-CO_3 used in the study. The broad band in the range of 3400–3500 cm^{-1} was assigned to ν_{OH} OH···HOH vibrations. The shoulder at 3000–3100 cm^{-1} was attributed to the OH vibrations of hydroxyl groups co-ordinated to the interlayer carbonate $OH{\cdot}CO_3^{2-}$ through hydrogen bonding. A bending vibration (δ_{H2O}) from the interlayer water is observed at 1600–1650 cm^{-1}. Carbonate anions peaks are observed at 850–880 cm^{-1} (ν_2), 1350–1380 cm^{-1} (ν_3) and 670–690 cm^{-1} (ν_4). These were assigned to non-planar bending, asymmetric stretching mode and bending angular mode respectively (Braterman *et al.*, 2004). However, these have been observed to split or shift to lower values if the symmetry of the carbonate anions is compromised. This is due to ionic and/or hydrogen bonding interaction of the CO_3^{2-} with the metal hydroxide lattice, hence interfering with the normal vibrations of the bonds. The position of the ν_3 peak (1370–1355 cm^{-1}) is sensitive to the M^{II}/M^{III} ratio. Costa *et al.* (2007) suggested that a strong electrostatic attraction between the interlayer anions is indicated by a decrease in the metal ratio (increase in the *x*-value). Hernendaz-Moreno *et al.* (1985) found that the ν_3 peak position shifted to lower wavenumbers with a decrease in the metal ratio, i.e. the M^{II}/M^{III} ratios equal to 3:1 and 2:1 had peaks positioned at 1370 and 1355 cm^{-1} respectively. The ν_3 peak was observed at 1358 cm^{-1} in this current study, which is in good agreement with the literature for an Mg^{2+}/Al^{3+} ratio that is close to 2:1.

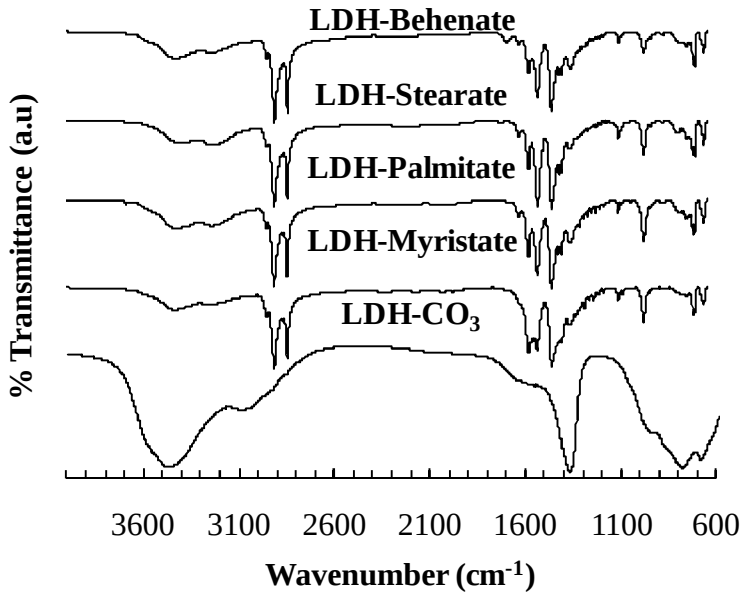

Figure 2.13. FTIR spectra of pristine and modified LDHs

The FTIR spectra were observed to vary for the different orientations of anions within the interlayer, i.e. monolayer or bilayer (Braterman *et al.*, 2004). A monolayer stearate-intercalated LDH was found to have two distinct peaks at 1549 cm^{-1}, attributed to the COO^- asymmetric stretching, and at 1412 cm^{-1} for the COO^- symmetric stretching. In the bilayer stearate-intercalated Zn_3Al-LDH, peaks were observed at 1597 cm^{-1} with shoulders at 1620 and 1398 cm^{-1}; these were assigned to H-bonded COOH vibration (Braterman *et al.*, 2004). Figure 2.13 shows the spectra of the fatty acid-modified LDHs. The observed spectra are typical for a bilayer fatty acid-intercalated LDH. The different fatty acid:LDH derivatives had similar spectra. The broad band between 3447 and 3391 cm^{-1} was assigned to hydroxyl groups on the LDH lattice and the presence of the intercalated water molecules. However, it is clear to see this particular peak becomes very broad and somewhat weak in the fatty acid-intercalated LDH as compared with the pristine LDH. This may be explained by the exclusion of a sizable quantity of intercalated water molecules due to the hydrophobisation of the interlayer by the fatty acids. A more detailed view of the peaks present and their exact positions is given in Figure 2.14.

The peaks in the fatty acid intercalated product in the regions 2956, 2915 and 2848 cm^{-1} are attributed to CH_2 symmetric and asymmetric stretching modes. The $\upsilon_{as}CH_2$ band was observed at a substantially low wavenumber (2915 cm^{-1}), which is an indication of a highly ordered all-trans conformation. The bending vibration of the intercalated water, $\delta(\upsilon H_2O)$, was observed at 1636 cm^{-1}. Peaks at 1583 cm^{-1} were attributed to the carboxylic acids being intercalated in the –RCOOH form (Borja & Dutta, 1992). Carlino & Hudson (1994) assigned the 1535 cm^{-1} peak to the asymmetric stretching mode of ionised -$RCOO^-$. However, they found that this particular mode may be positioned anywhere within the range of 1558–1536 cm^{-1}. The asymmetric mode was observed by Perez-Ramirez *et al.* (2001) in the range of 1425–1411 cm^{-1}. In the current study these are detected as weak peaks at 1428 and 1411 cm^{-1}. A medium peak around 1466 cm^{-1} was attributed by Borja & Dutta (1992) to CH_2 bending of the carboxylic acid chain. This band was also found to be sensitive to interchain interactions and the packing arrangement (Vaia *et al.*, 1994). The LDH-myristate exhibits a much broader peak and a slightly lower wavenumber. This is an indication of an increase in the chain motion or liquid-like character of the fatty acid chains. The peak at 1368 cm^{-1} shows a broad and very weak band, which is an indication of a slight carbonate impurity.

The summation of the peaks observed is evidence of the presence of carboxylate within the interlayer. It also substantiates the fact that for a bilayer to form, the fatty acid should be intercalated in both an ionised and unionised fatty acid form (Kuehn & Poellman, 2010).

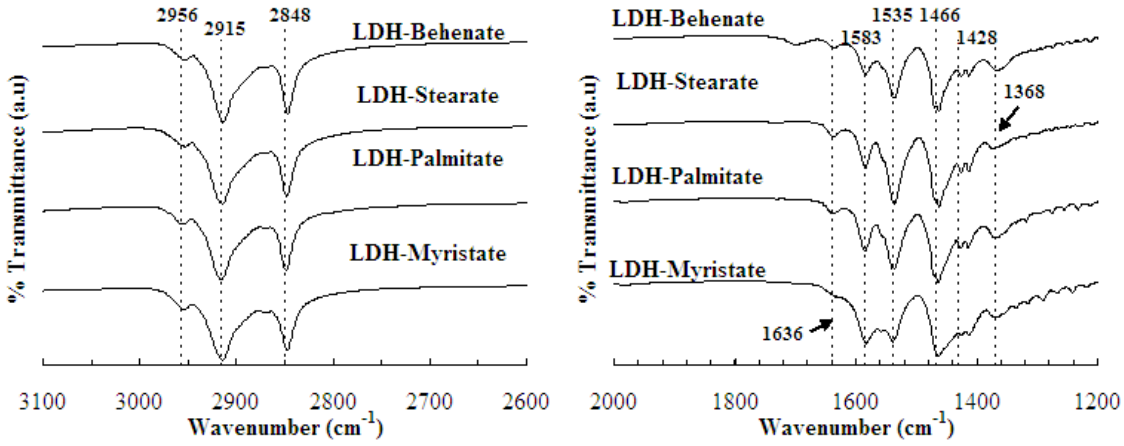

Figure 2.14. FTIR zoom of the modified LDH

2.6.4 Thermal analysis

The thermal behaviour, stability and decomposition pathways of the organo-LDH hybrids were studied by means of DSC, temperature scan FTIR and XRD, TG and TG-FTIR.

2.6.4.1 Differential scanning calorimetry (DSC)

In Figure 2.15 the red dotted and solid black lines denote the neat fatty acid and intercalated LDHs respectively. The DSC scans of the organo-LDH show that the intercalation of the fatty acids results in a shift of the melting temperature to a higher temperature. The confinement of the fatty acids within the LDH layers prevents their premature melting. All the intercalated samples exhibit two or three endotherms, which may be attributed to the different phase transitions undergone by the bilayer intercalated LDH as the temperature increased. The multiple peaks could be an indication of mixed layers as already indicated in the EDS results, where the ratios of Mg to Al vary from platelet to platelet. Another contributing factor to the peaks observed is the water of hydration of the organo-LDH.

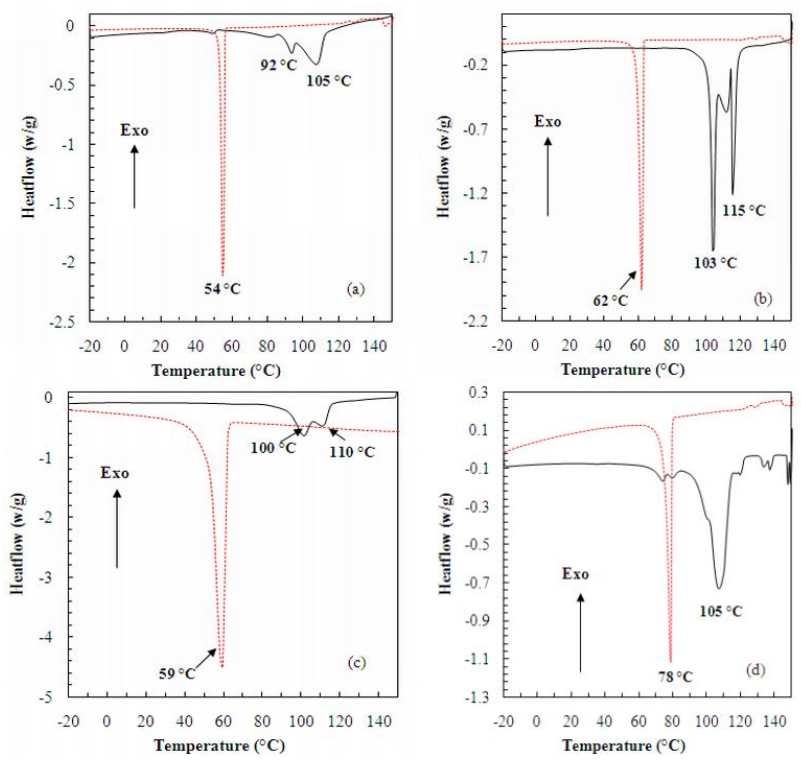

Figure 2.15. DSC traces of neat fatty acids in red and LDH-fatty acids as a solid line: (a) myristate, (b) palmitate, (c) stearate and (d) behenate

The dominant peaks have been assigned to the melting of the interlayer anions. It is clear from the traces that there is a slight fatty acid impurity for the LDH-stearate and -behenate samples.

2.6.4.2 Temperature scan XRD and FTIR

Figure 2.16 shows the effect of temperature on the crystal structure. Generally, the fatty acid-intercalated LDH has the primary basal reflection shifting to higher 2θ values, indicating a reduction in the d-spacing. The first shift to lower 2θ values is due to the removal of interlayer water, accompanied by a reduction in the d-spacing of 0.3 nm (Pesic *et al.*, 1994). At temperatures higher than 120 °C, another transition occurs, which is accompanied by the disappearance of the 2nd and 3rd reflections. The primary reflection either broadens progressively or disappears completely with increase in temperature; this is attributed to the organo-LDH becoming amorphous. The LDH-stearate exhibits reductions in the basal spacing from 4.98 to 4.26 to 2.92 nm at 25, 90 and 150 °C respectively. The last spacing is consistent with a monolayer arrangement. Similar transitions were observed in the LDH-palmitate with the changes in d-spacing being 4.46 to 4.05 to 2.76 nm at 25, 120 and 200 °C respectively. These transitions, however, were difficult to follow due to peak broadening and disappearance in the LDH-behenate. The LDH-myristate, however, showed an increase in the d-spacing; this deviation from the normal trend is still not fully understood. Dutta & Borja (1992), however, observed a similar phenomenon in myristate-intercalated Li-Mg LDH.

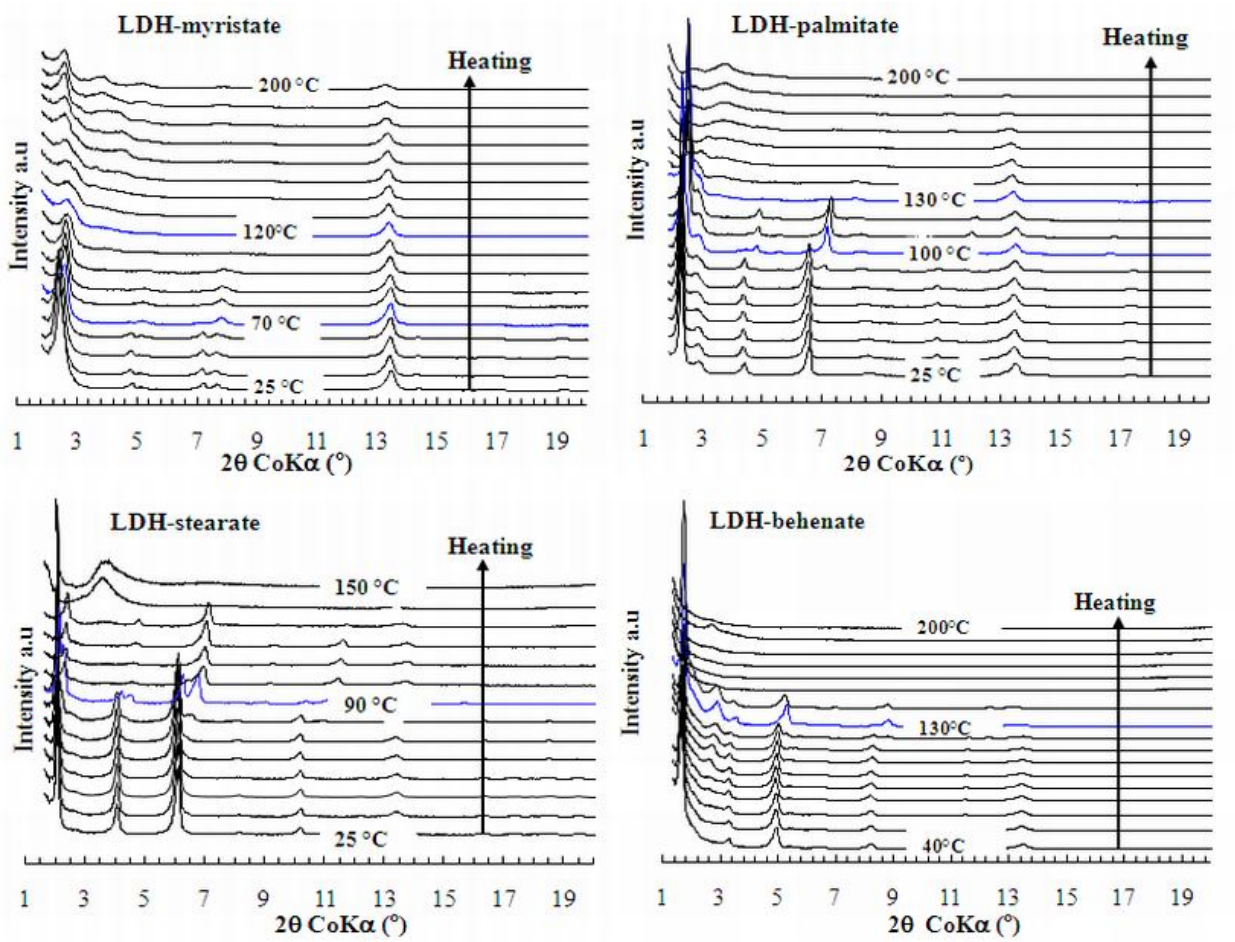

Figure 2.16. Temperature scan XRD of LDH-fatty acids

LDH-stearate was used to further illustrate the thermotropic behaviour of LDH-carboxylate. Figure 2.17 shows the effect of temperature on the peak position of the $\upsilon_{as}(CH_2)$ band in the FTIR spectra. Vaia *et al.* (1994) proposed that the wavenumber and width of the above-mentioned band are sensitive to the gauche trans conformer ratio and the packing density of the methylene chains. This band ranges from 2917 to 2929 cm^{-1} for the methylene chains in the all-trans ordered state and when in a liquid-like environment respectively. It showed a shift from values observed for crystalline well-ordered chains (2916.8 cm^{-1}) to higher values of 2925 cm^{-1}. This is consistent with an increase in conformational disorder in the intercalated chains as the temperature increases. The intermediate wavenumber values (2924 cm^{-1}) obtained in our study suggest that the chains still retained a degree of order above the transition temperature, i.e. that they are not completely molten. The investigation also revealed a greater amount of disorder for short-chain fatty acids (laurate) as compared with longer stearate chains (Focke *et al.*, 2010).

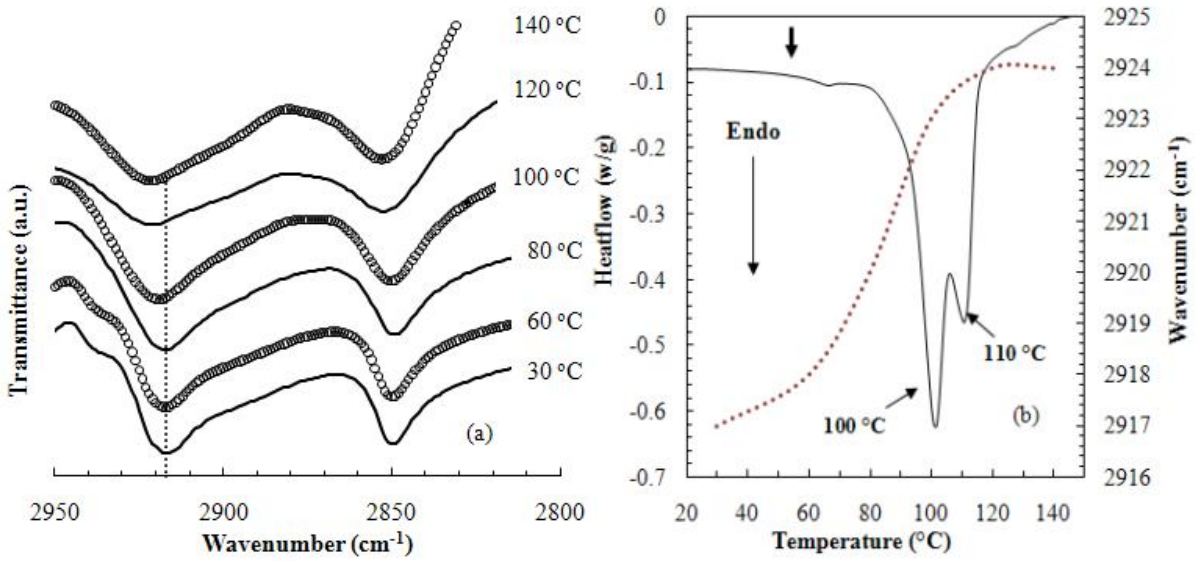

Figure 2.17. Effect of temperature on the peak position of the $\upsilon_{as}(CH_2)$ band in the FTIR spectra for LDH-stearate, and the corresponding DSC

From Figure 2.17 it is clear that following the phase changes through temperature scan FTIR is a more sensitive method than following them through XRD. It is evident that the movement of intercalated anions begins at much lower temperatures (≈ 45 °C) as observed in FTIR, whereas in XRD the movement is clearly seen at a much higher temperatures (≈ 90 °C).

2.6.4.3 Decomposition pathway of organo-LDH

The decomposition pathways of LDH and its derivatives were followed by means of TGA (Figure 2.18). The organic content was also derived from these results. The calculation is based on the differences in mass observed at temperatures of 150 and 900 °C relative to the corresponding values for the LDH-CO_3 precursor. A detailed calculation for the degree of intercalation appears in Appendix B, along with the results of the other trials. Pristine LDH-CO_3 follows three distinct steps, i.e. dehydration, dehydroxylation and elimination of interlayer anions. The temperatures at which each of the individual events occur varies with different metal ion species and ratios (Ross & Kodama, 1967), intercalated anions (Xu & Zheng, 2001; Mascolo & Marino, 1982) and post-treatment of the LDH (Hussein *et al.*, 2000). The different stages observed in this study fit well with the decomposition pathway of (Mg-Al)-LDH-CO_3 as proposed by Bera *et al.* (2000):

I $Mg_{(1-x)}Al_x(OH)_2(CO_3^{2-})_{x/2}\cdot mH_2O \longrightarrow Mg_{(1-x)}Al_x(OH)_2(CO_3^{2-})_{x/2} + mH_2O\uparrow$

II $Mg_{(1-x)}Al_x(OH)_2(CO_3^{2-})_{x/2} \longrightarrow x/2MgAl_2O_4 + (1-{}^{3x}/_2)\ MgO + H_2O\uparrow + CO_2\uparrow$

III $x/2MgAl_2O_4 + (1-{}^{3x}/_2)\ MgO \longrightarrow MgO + Al_2O_3$

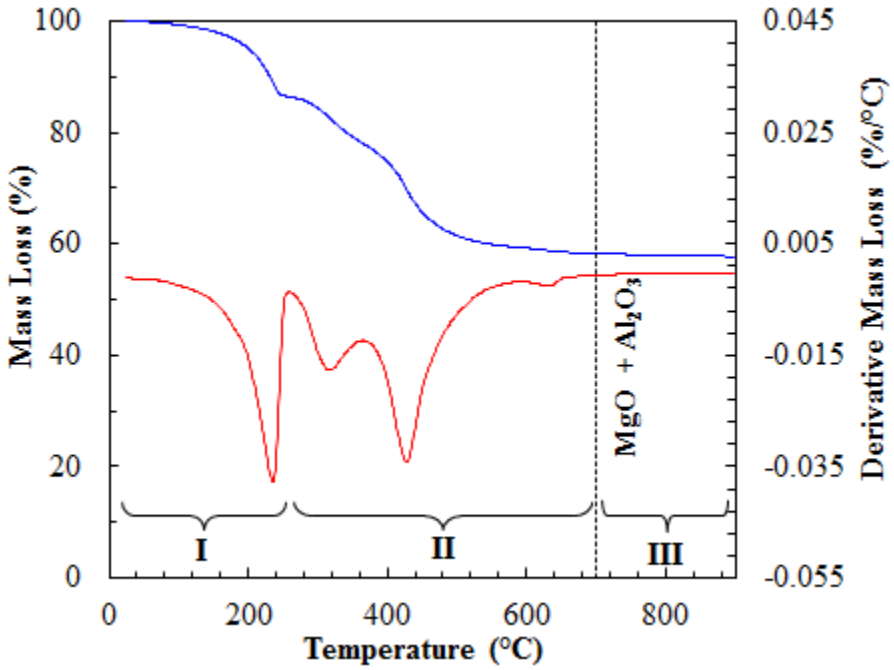

Figure 2.18. TG and DTG of the LDH-CO_3 indicating the different decomposition stages

The first event is usually assigned to the loss of physiosorbed interlayer water. The onset of this step begins at about 50 °C and is perceived to be complete at 150 °C (Carlino & Hudson 1994; Kandare and Hossenlopp, 2006; Frost *et al.* 2003). The second step is due to a dehydroxylation process, immediately followed by an oxidative degradation of the carbonate anions within the interlayer, with the former occurring at about 280 °C and the latter above 450 °C.

The difference in mass loss between the LDH-CO_3 and the fatty acid modified LDH was used to calculate the percentage organic and the AEC level (Figure 2.19a). The percentages organic for each respective organo-LDH were as follows: 74, 73, 79 and 81% for LDH-myristate, -palmitate, -stearate and -behenate respectively. The modified LDHs appear to follow the same decomposition pattern as the pristine LDH-CO_3 (Figure 2.19b). It is evident

that the breakdown of the hydroxyl lattice and degradation of anions occurs at temperatures above 280 °C, well above polymer processing temperatures. Mass loss is effectively complete above 700 °C, leaving a residue of MgO and Al_2O_3. The water loss occurs at substantially lower temperatures than with the LDH-CO_3. However, the dehydroxylation process seems to occur simultaneously with the removal of anions (de-anionation). LDH-behenate showed a higher decomposition temperature peak and LDH-myristate the lowest.

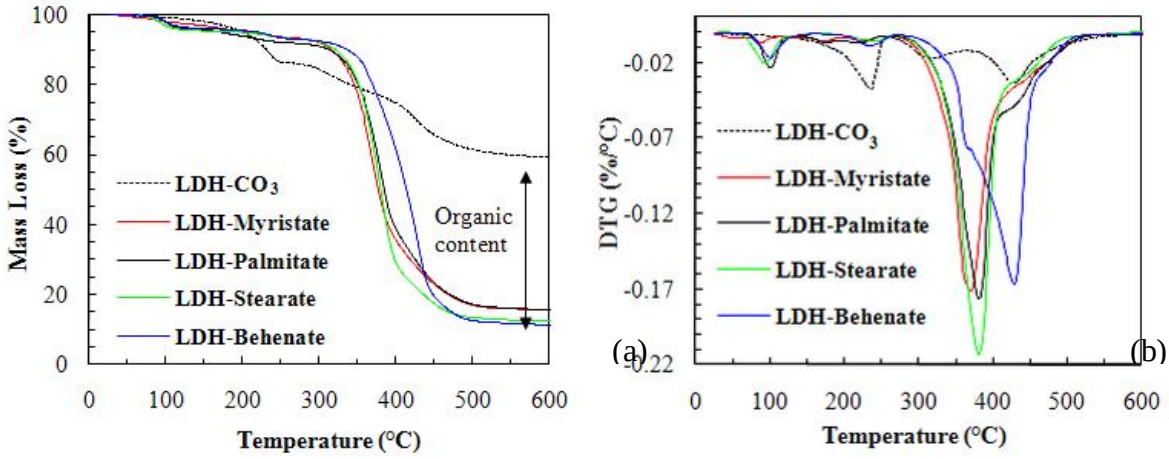

Figure 2.19. Thermogravimetic analysis: (a) % mass loss and (b) derivative mass loss of pristine and modified LDHs

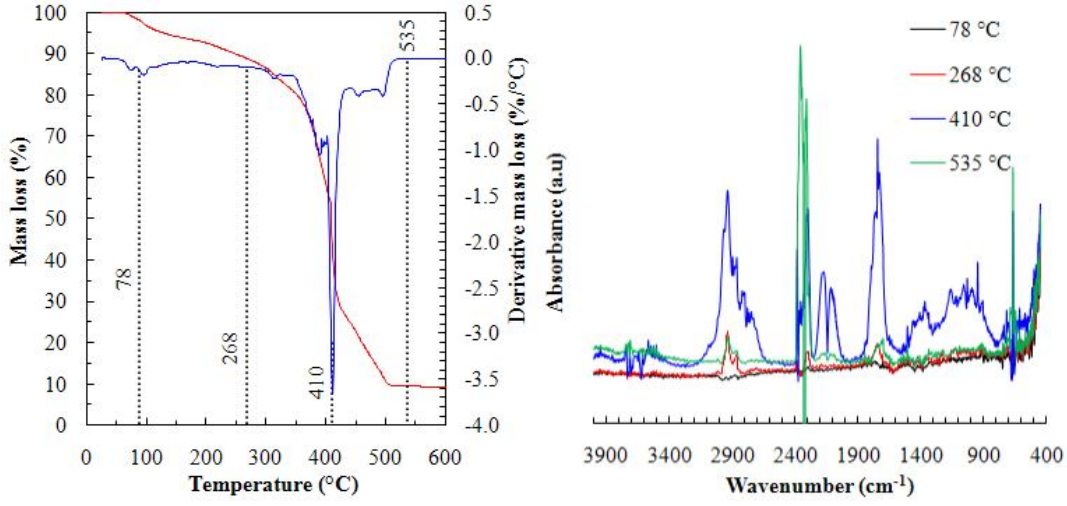

Figure 2.20. Evolved gas analysis for LDH-stearate

To confirm the decomposition pathway, evolved gas analysis was carried out by means of TG-FTIR (Figure 2.20). The water loss is, however, not detected by the FTIR. The regions that would exhibit water peaks (3700–3400 cm^{-1}) are characterised by noise-like signals on the spectra. Decomposition of the LDH-stearate begins at about 268 °C. Methylene groups

(2943 cm^{-1}) and CO_2 asymmetric stretching (2385–2303 cm^{-1}) are detected, but the intensities of the peaks are weak. At 410 °C the peak intensities are relatively larger and were distinguished as follows: alkyl groups CH-symmetric and asymmetric stretching (2943 cm^{-1}), 2385–2303 cm^{-1}; 2193 and 2162 cm^{-1} peaks are assigned to CO vibrations; 1743 cm^{-1} was attributed to carboxylic acid groups C=O stretching vibration; and CH bending vibrations are picked up at 1412 cm^{-1}. The carbonyl species are identified in the range of 1545–882 cm^{-1} by a very broad peak. At around 535 °C only a CO_2 peak was present.

Table 2.5. Summary of thermogravimetric data and estimates for the degree of intercalation

Sample identity	Residual mass loss (%) at		Carboxylate:Al mol ratio
	150 °C	900 °C	
LDH-CO_3	98.10	57.68	-
LDH-myristate	96.88	14.61	2.64
LDH-palmitate	95.73	14.92	2.24
LDH-stearate	95.40	13.11	2.39
LDH-behenate	96.04	10.72	2.60

The thermogravimetric data and estimates of the degree of carboxylate intercalation are summarised in Table 2.5. Nhlapo *et al.* (2008) calculated the theoretical possible amount to be 2.39 times the AEC for close-packed carboxylate chains. It is evident that intercalation occurs at higher than the AEC expected for LDHs, implying that the excess exists as un-ionised fatty acids. It is worth noting that the TGA data indicates variable levels of intercalation amongst the different batches prepared in this study (compare Tables 2.5, 2.6, B6 and B7). This could be explained by changes in the pH during modification due to the evaporation of ammonia and inadequate/too many washes.

A complete conversion of the LDH-CO_3 precursor to magnesium distearate and aluminium tristearate would result in an apparent degree of intercalation of 6.93. The magnesium/aluminium stearate sample was synthesised in order to explore this possibility. Figure 2.21 compares the XRD diffractograms of this product with those of the two precursors. It clearly shows that heating these two stearates together results in a new product with a larger d-spacing. The TGA data shown in Table 2.6 indicate that there was a net loss of stearic acid. There is also an indication that not all of the aluminium stearate was converted. Furthermore, it is clear that the product is not a simple LDH-stearate but rather a

mixed magnesium/aluminium stearate with a d-spacing that is very similar to that of bilayer-intercalated LDH. This experiment confirms that such a compound can form through partial hydrolysis of the metal stearates. It is therefore conceivable that LDH-stearates that have an exceptionally high AEC and may contain mixed layers of such a product, as well as the conventional LDH-stearate. The EDS analysis (Figure 2.9) of the LDH-palmitate with an AEC of 2.24 shows areas that have the correct Mg:Al ratios, as well as some platelets that are either Mg-rich or Al-rich.

Table 2.6. Summary of XRD and TGA results for the LDH-CO_3, LDH-stearates and magnesium stearate and aluminium stearate samples

Sample	d-spacing (nm)	TG residue* (wt%)	Intercalation** (multiples of AEC)
LDH-CO_3	0.76	59.7	-
LDH-CO_3 + Tween 60	0.76	58.4	-
LDH-stearate	4.88	10.23	3.87
Magnesium/aluminium stearate	5.08	8.23	5.16
Magnesium stearate	4.94	7.30	(5.70)
Aluminium stearate	4.01	8.57	(5.11)

*Mass loss at 700 °C relative to the mass loss at 150 °C

**Apparent degree of stearate intercalation expressed as multiples of AEC, assuming that the basis is an LDH clay

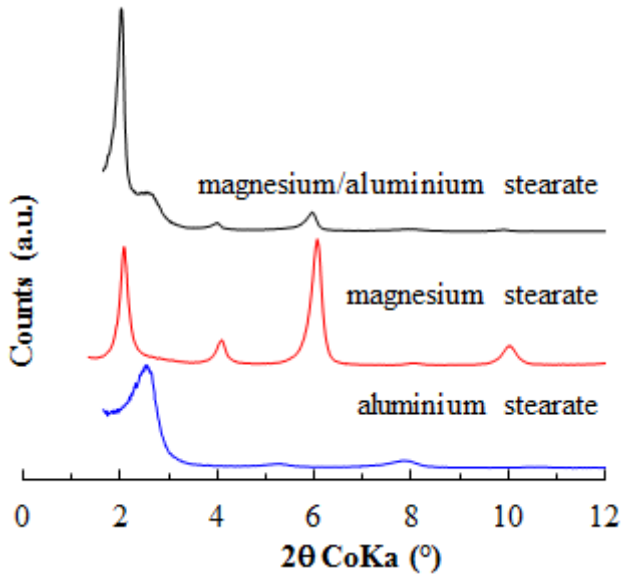

Figure 2.21. X-ray diffractograms for magnesium stearate, aluminium stearate and magnesium/aluminium stearate prepared by heating an aqueous suspension of the former two reagents in the presence of Tween 60

2.7 CONCLUSIONS

The carboxylate intercalated LDHs were successfully obtained from direct ion exchange of the fatty acid with the interlayer carbonate. The method employed is reproducible with respect to a bilayer intercalated product. It is evident from the FTIR results and the high AEC of intercalated fatty acids that in bilayers orientation will always co-intercalate the carboxylates, as well as the free fatty acid molecules. The incorporation of excess fatty acids is envisaged to be driven by hydrophobic interactions. The presence of the free fatty acids facilitates dense packing, improving the van der Waals interaction between the chains and giving better charge shielding of the same-charge surfactant head group. The high degree of chain order leads to more efficient packing and increased cohesive van der Waals interaction between chains and, ultimately, to a greater interlayer solid-like character as observed in FTIR analysis.

The fatty acid-intercalated LDHs showed structural changes as a function of temperature. They undergo melt-like transitions at elevated temperatures. Above the melting point they assume a liquid-crystalline ‘rotator’ state owing to the localisation of the ionised head group and the two-dimensional confinement imposed by the planar clay sheets. Hence, this event is followed by a reduction in the d-spacing. At higher temperatures the LDH-fatty acid-based materials become XRD-amorphous: basal reflections disappear or become very broad. The LDH-stearate and -palmitate clearly showed a reduction in d-spacing, where the bilayer arrangement collapses to a monolayer.

The study also revealed that various intercalation products can be obtained from the one-pot synthesis as shown by the EDS results. Platelets with different Mg/Al ratios were observed specifically in the well-crystallised LDH-palmitate. This is an indication that the method employed entailed dissolution and recrystallisation of the pristine LDH and organo-LDH respectively. It is further substantiated by changes in the platelet morphology (from subhedral to rhombohedral-shaped platelets) and size. The unusually high AEC values obtained for some of the fatty acid-intercalated LDHs are attributed to the formation of Mg- and Al-rich platelets.

2.8 REFERENCES

Abelló, S. & Pérez-Ramírez, J. (2006). Steam activation of Mg–Al hydrotalcite. Influence on the properties of the derived mixed oxides. *Microporous Mesoporous Mater.*, 96(1–3): 102–108.

Adachi-Pagano, M., Forano, C. & Besse J-P. (2003). Synthesis of Al-rich hydrotalcite-like compounds by using the urea hydrolysis reaction – control of size and morphology. *J. Mater. Chem.*, 13: 1988–1993.

Aramendia, M. A., Borau, V., Jimenez, C., Marinas, J. M., Ruiz, J. R. & Urbano, F. J. (2002). Comparative study of Mg/M(III) (M=Al, Ga, In) layered double hydroxides obtained by coprecipitation and the sol-gel method, *J. Solid State Chem.*, 168: 156–161.

Bera, P., Rajamathi, M., & Hegde, M. S. (2000). Thermal behaviour of hydroxides, hydroxysalts and hydrotalcites, *23*(2): 141–145.

Boclair, J. W. & Braterman, P. S. (1999). Layered double hydroxide stability. 1. Relative stabilities of layered double hydroxides and their simple counterparts. *Chem. Mater.*, 11: 298–302.

Borja, M. & Dutta, P. K. (1992). Fatty acids in layered metal hydroxides: Membrane-like structure and dynamics. *J. Phys. Chem.* 96: 5434–5444.

Braterman, P. S., Xu, Z.P. & Yarberry, F. (2004). In: Auerbach, S.M., Carrado, K. A. & Dutta, P. K. (Eds), *Handbook of Layered Materials*, Boca Raton: CSC Press, Taylor & Francis Group, pp 373–449.

Brindley, G. W. & Kikkawa, S. (1979). A crystal-chemical study of Mg,Al and Ni,Al hydroxy-perchlorates and hydroxy-carbonates. *Am. Mineral.*, 64: 836–843.

Carlino, S. & Hudson, M. J. (1994). The reaction of molten sebacic acid with a layered (Mg/Al) double hydroxide. *J. Mater. Chem.*, 4: 99–104.

Carlino, S. (1997). The intercalation of carboxylic acids into layered double hydroxides: A critical evaluation and review of different methods. *Solid State Ionics*, 98: 73–84.

Cavani, F., Trifirò, F. & Vaccari, A. (1991). Hydrotalcite-type anionic clays: Preparation, properties and applications. *Catal. Today*, 11: 173–301.

Chibwe, K. & Jones, W. (1989). Intercalation of organic and inorganic anions into layered double hydroxide. *J. Chem. Soc., Chem. Commun.*, 926–927.

Constantino, V. R. L. & Pinnavaia, T. J. (1995). Basic properties of $Mg^{2+}_{1-x}Al^{3+}_{x}$ layered double hydroxides intercalated by carbonate, hydroxide, chloride and sulfate anions. *Inorg. Chem.*, 34: 883–892.

Costa, F. R., Leuteritz, A., Meinl, J., Wagenknecht, U. & Heinrich, G. (2011). LDH as nanofiller: Organic modification and dispersion in polymers. *Macromolecular Symposia*, 301(1): 46–54.

Costa, F. R., Leuteritz, A., Wagenknecht, U., Jehnichen, D., Häusler, L. & Heinrich, G. (2008). Intercalation of Mg-Al layered double hydroxides by anionic surfactants: Preparation and characterization. *Appl. Clay. Sci.*, 38(3-4): 153–164.

Costa, F. R., Wagenknecht, U. & Heinrich, G. (2007). LDPE/Mg–Al layered double hydroxide nanocomposite: Thermal and flammability properties. *Polym. Degrad. Stab.*, 92(10), 1813–1823.

Costa, F. R., Wagenknecht, U., Jehnichen, D., Abdel-Goad, M. & Heinrich, G. (2006). Nanocomposites based on polyethylene and Mg-Al layered double hydroxide. Part II: Rheological characterization. *Polymer*, 47: 1649–1660.

Crepaldi, E. L., Pavan, P. C. & Valim, J. B. (1999). A new method of intercalation by anion exchange in layered double hydroxides. *Chem. Commun.*, 155–156.

Crepaldi, E. L., Tronto, J., Cardoso, L. P. & Valim, J. B. (2002). Sorption of terephalate anions by calcined and uncalcined hydrotalcite-like compounds. *Colloids Surf. A.*, 211: 103–114.

Delmas, C. & Borthomieu, Y. (1993). Chimie douce reaction: A new route to obtain well crystallized layered double hydroxides. *J. Solid State Chem.*, 104: 345–352.

Feitknecht, W. & Gerber, M. (1942). Zur Kenntnis der Doppelhydroxide und der basichen Doppelsalze (III). *Helv Chim Acta.*, 25: 131–137.

Focke, W. W., Nhlapo, N. S., Moyo, L. & Verryn, S. M. C. (2010). Thermal properties of lauric- and stearic acid intercalated layered double hydroxides. *Mol. Cryst. Liq.Cryst.*, 521(1): 168–178.

Forano, C., Hibino, T., Leroux, F. & Taviot-Gueho, C. (2006). Layered double hydroxides. In: Bergaya, F., Theng, B. K. G. & Lagaly, G. (Eds.), *Handbook of Clay Science*, Amsterdam: Elsevier, pp 1021-1095

Frost, R. L., Martens, W., Ding, Z. & Kloprogge, J. T. (2003). DSC and high-resolution TG of synthesized hydrotalcites of Mg and Zn. *J. Therm. Anal. Calorim.*, 71: 429–438.

Grim, R.E. & Güven, N. (1978). *Bentonites: Geology, Mineralogy, Properties and Uses*. Amsterdam and New York: Elsevier, p 256.

Grover, K., Komarneni, S. & Katsuki, H. (2010). Synthetic hydrotalcite-type and hydrocalumite-type layered double hydroxides for arsenate uptake. *Appl. Clay. Sci.*, 48(4): 631–637.

He, J., Wei, M., Li, B., Kang, Y., Evans, D. G. & Duan, X. (2005). Preparation of layered double hydroxides. In: Evans, D. G. & Duan, X. (Eds). *Layered Double Hydroxides*, Heidelberg, Germany: Springer, pp 89–119.

Hernandez-Moreno, M. J., Ulibarri, M. A., Rendon, J. L. & Serna, C. J. (1985). IR characteristics of hydrotalcite-like compounds. *Phys. Chem. Miner.*, 12: 34–38.

Hibino, T. & Tsunashima, A. (1998). Characterization of repeatedly reconstructed Mg-Al hydrotalcite-like compounds: Gradual segregation of aluminum from the structure. *Chem. Mater.*, 10: 4055–4061.

Hussein, M. Z. B., Zainal, Z. & Ming, C. Y. (2000). Microwave-assisted synthesis of Zn-Al-layered double hydroxide-sodium dodecyl sulfate nanocomposites. *J. Mater. Sci. Lett.*, 19: 879–883.

Ikeda, T., Amoh, H. & Yasunaga, T. (1984). Stereoselective exchange kinetics of L- and D-histidines for Cl− in the interlayer of a hydrotalcite-like compound by the chemical relaxation method. *J. Am. Chem. Soc*, 106, 5772–5775.

Indira, L., Dixit, M., & Kamath, P. V. (1994). Electrosynthesis of layered double hydroxides of nickel with trivalent cations. *Journal of Power Sources*, *52*(1): 93–97.

Itoh, T., Ohta, N., Shichi, T., Yui, T. & Takagi, K. (2003). The self-assembling properties of stearate ions in hydrotalcite clay composites. *Langmuir*, 19: 9120–9126.

Iyi, N. & Sasaki, T. (2008). Decarbonation of MgAl-LDHs (layered double hydroxides) using acetate-buffer/NaCl mixed solution. *J. Colloid Interface Sci.*, 322: 237–245.

Iyi, N., Matsumoto, T., Kaneko, Y. & Kitamura, K. (2004). Deintercalation of carbonate ions from a hydrotalcite-like compound: Enhanced decarbonation using acid-salt mixed solution. *Chem. Mater.*, 16: 2926–2932.

Iyi, N., Okamoto, K., Kaneko, Y. & Matsumoto, T. (2005). Effects of anion species on deintercalation of carbonate ions from hydrotalcite-like compounds. *Chem. Lett.*, 34: 932–933.

Jitianu, M., Zaharescu, M., Balasoiu, M. & Jitianu, A. (2003). The sol-gel route in synthesis of Cr(III)-containing clays. Comparison between Mg-Cr and Ni-Cr anionic clays. *J. Sol-Gel Sci. Technol.*, 26: 217–221.

Kandare, E. & Hossenlopp, J. M. (2006). Thermal degradation of acetate-intercalated hydroxy double and layered hydroxy salts. *Inorg. Chem.*, 45: 3766–3773.

Kanicky, J. R. & Shah, D.O. (2002). Effect of degree, type, and position of unsaturation on the pKa of long-chain fatty acids. *J. Colloid Interface Sci.*, 207: 201–207.

Kannan, S., Jasra, R. V. & Salt, C. (2000). Microwave-assisted rapid crystallization of Mg-M(III) hydrotalcite where M(III) = Al, Fe or Cr. *J. Mater. Chem.*, 10: 2311–2314.

Kanoh, T., Shichi, T. & Takagi, K. (1999). Mono- and bilayer equilibria of stearate self-assembly formed in hydrotalcite interlayers by changing the intercalation temperature. *Chem. Lett.*: 117–118.

Khan, A. & O'Hare, D. (2002). Intercalation chemistry of layered double hydroxides: Recent developments and applications. *J. Mater. Chem.*, 12: 3191–3198.

Kooli, F., Kosuge, K. & Tsunashima, A. (1995). New Ni-Al-Cr and Ni-Al-Fe carbonate hydrotalcite-like compounds: Synthesis and characterization. *J. Solid State Chem.*, 118: 285–291.

Kuehn, T, Poellmann H. (2010). Synthesis and characterization of Zn-Al layered double hydroxides intercalated with 1- to 19-carbon carboxylic acid anions. *Clays Clay Miner.*, 58(5): 596–605.

Landman, E. P. (2005) Stearate intercalated layered double hydroxides: Methods and application. PhD thesis, Pretoria: University of Pretoria.

Latterini, L., Elisei, F., Aloisi, G. G., Costantino, U. & Nocchetti, M. (2002). Space-resolved fluorescence properties of phenolphthalein-hydrotalcite nanocomposites. *Phys. Chem. Chem. Phys.*, 4(12): 2792–2798.

Lopez, T., Bosch, P., Ramos, E., Gomez, R., Novaro, O. & Acosta, D. (1996). Synthesis and characterization of sol-gel hydrotalcites. Structure and texture. *Langmuir*, 189–192.

Lotsch, B., Walton, R., O'Hare, D. & Millange, F. (2001). Separation of nucleoside monophosphates using preferential anion exchange intercalation in layered double hydroxides. *Solid State Science*, 3(8): 883–886.

Mascolo, G. & Marino, O. (1980). A new synthesis and characterization of magnesium-aluminium hydroxides. *Miner. Mag.*, 43: 619–621.

Mascolo, G. (1995). Synthesis of anionic clays by hydrothermal crystallization of amorphous precursors. *Appl. Clay Sci.*, *10*(1-2): 21–30.

McMurry, J. (2000). *Organic Chemistry*, 5th edition. USA: Thomson Brooks/Cole, p 1284.

Meyn, M., Beneke, K. & Lagaly, G. (1990). Anion-exchange reactions of layered double hydroxides. *Inorg. Chem.*, 29: 5201–5207.

Miyata, S & Okada, A .(1977). Synthesis of hydrotalcite-like compounds and their physico-chemical properties – the systems $Mg^{2+}Al^{3+}$-SO_4^{2-} and $Mg^{2+}Al^{3+}$-CrO_4^{2-}. *Clays Clay Miner.*, 25: 14–18.

Miyata, S. & Kumura, T. (1973). Synthesis of new hydrotalcite-like compounds and their physico-chemical properties. *Chem. Lett.*, 843–848.

Miyata, S. (1980). Physico-chemical properties of synthetic hydrotalcites in relation to composition. *Clays Clay Miner.*, 28: 50–56.

Moyo L. (2009) A critical assessment of the methods for intercalating anionic surfactants in layered double hydroxides. MSc dissertation, Pretoria: University of Pretoria.

Moyo, L., Focke, W. W., Labuschagne F.J. & Verryn, S. (2012) Layered double hydroxide intercalated with sodium dodecyl sulphate. *Mol. Cryst. Liq.Cryst.*, 555(1): 51–64.

Moyo, L., Nhlapo, N. S. & Focke, W. W. (2008). A critical assessment of the methods for intercalating anionic surfactants in layered double hydroxides. *J. Mater. Sci.*, 43: 6144–6158.

Nhlapo, N., Motumi, T., Landman, E., Verryn, S. M. C. & Focke, W. W. (2008). Hydrotalcite: Surfactant-assisted fatty acid intercalation of layered double hydroxides. *J. Mater. Sci.*, 43(3): 1033–1043.

Nyambo, C., Chen, D., Su, S. & Wilkie, C. (2009). Does organic modification of layered double hydroxides improve the fire performance of PMMA? *Polym. Degrad. Stab.*, 94(8): 1298–1306.

O'Hare, D. (1991). Inorganic intercalation compounds. In: Bruce, D. W. & O'Hare, D. (Eds), *Inorganic Materials*, New York: Wiley, pp 166–228.

Othman, M. R., Helwani, Z. & Fernando, W. J. N. (2009). Synthetic hydrotalcites from different routes and their application as catalysts and gas adsorbents: A review. *Appl. Organomet. Chem.*, 23(9), 335–346.

Perez-Ramirez, J., Mul, G., Kapteijn, F. & Moulijn, J. A. (2001). A spectroscopic study of the effect of the trivalent cation on the thermal decomposition behaviour of Co-based hydrotalcites. *J. Mater. Chem.*, 11: 2529–2536.

Pesic, L., Salipurovic, S., Markovic, V., Vucelic, D., Kagunya, W., & Jones, W. (1992). Thermal characteristics of a synthetic hydrotalcite-like material. *J. Mater. Chem.*, *2*(10): 1069.

Prinetto, F., Ghiotti, G., Graffin, P. and Tichit, D. (2000). Synthesis and characterization of sol-gel Mg/Al and Ni/Al layered double hydroxides and comparison with co-precipitated samples. *Microporous Mesoporous Mater.*, 39: 229-247.

Ramos, E., Lopez, T., Bosch, P., Asomoza, M. & Gomez, R. (1997). Thermal stability of sol-gel hydrotalcites. *J. Sol-Gel Sci. Technol.*, 8: 437–442.

Rao, M. M., Reddy, B. R., Jayalakshmi, M., Jaya, V. S. & Sridhar, B. (2005). Hydrothermal synthesis of Mg–Al hydrotalcites by urea hydrolysis. *Mater. Res. Bull.*, 40: 347–359.

Rocha, J., Arco, M. D., Rives, V. & Ulibarri, M. (1999). Reconstruction of layered double hydroxides from calcined precursors: a powder XRD and 27Al MAS NMR study. *J. Mater. Chem.*, 3(1 M): 2499–2503.

Ross, G.J. & Kodama, H. (1967) Properties of a synthetic magnesium-aluminum carbonate hydroxide and its relationship to magnesium-aluminum double hydroxide, manasseite and hydrotalcite. *Amer. Miner.*, 52: 1036–1047.

Sato, T., Tezuka, M., Endo, T. & Shimada, M. (1988). Removal of sulfuroxyanions by magnesium aluminium oxides and their thermal decomposition. *J. Chem. Tech. Biotechnol.*, 39: 275–285.

Stanimirova, T. S., Kirov, G. & Dinolova, E. (2001). Mechanism of hydrotalcite regeneration. *J. Mat. Sci. Lett.*, 20: 453–455.

Sugimoto, A., Ishida, S., & Hanawa, K. (1999). Preparation and Characterization of Ni/Al-Layered Double Hydroxide. *J. Electrochem. Soc.*, *146*(4): 1251–1255.

Trifiro, F. & Vaccari, A. (1996). Hydrotalcite-like anionic clays (layered double hydroxides). In: Davies, J. E. D., Atwood, J. L., MacNicol, D. D. & Vogtle, F. (Eds), *Comprehensive Supramolecular Chemistry*, Oxford, UK: Pergamon Press, pp 251–291.

Utracki, L. A., Sepehr, M. & Boccaleri, E. (2007). Synthetic, layered nanoparticles for polymeric nanocomposites (PNCs). *Polym. Adv. Technol.*, 18(1): 1–37.

Vaia, R. A., Teukolsky, R. K. & Giannelis, E. P. (1994). Interlayer structure and molecular environment of alkylammonium layered silicates. *Chem. Mater.*, 6(16): 1017–1022.

Whitesides, G. M., Mathias, J. P. & Seto, C. T. (1991). Molecular self-assembly and nanochemistry: A chemical strategy for the synthesis of nanostructures. *Science*, 254: 1312–1319.

Xiang, X., Zhang, L., Hima, H. I., Li, F. & Evans, D. G. (2009). Co-based catalysts from Co/Fe/Al layered double hydroxides for preparation of carbon nanotubes. *Appl. Clay Sci.*, 42(3–4): 404–409.

Xu, Z. P & Braterman, P. (2010). Synthesis, structure and morphology of organic layered double hydroxides (LDH) hybrids: Comparison between aliphatic and their oxygenated analogs. *Appl. Clay Sci.*, 48: 235–242.

Xu, Z. P. & Zeng, H. C. (2001). Decomposition pathways of hydrotalcite-like compounds $MgAl_x(OH)_2(NO_3)_x{\cdot}nH_2O$ as a continuous function of nitrate anions. *Chem. Mater.*, 13: 4555–4563.

Yang, Z., Choi, K.-M., Jiang, N. & Park, S.-E. (2007). Microwave synthesis of hydrotalcite by urea hydrolysis. *Bull. Korean Chem. Soc.*, 28(11): 2029–2033.

Zaneva, S. & Staminirova, T. (2004). Crystal chemistry, classification position and nomenclature of layered double hydroxides. Bulgarian Geological Society, Annual Scientific Conference.

Zhang, P., Qian, G., Xu, Z. P., Shi, H., Ruan, X., Yang, J. & Frost, R. L. (2012). Effective adsorption of sodium dodecylsulfate (SDS) by hydrocalumite (CaAl-LDH-Cl) induced by self-dissolution and re-precipitation mechanism. *J. Colloid Interface Sci.*, 367(1): 264–71.